GRAPHENE BASED SURFACE PLASMON POLARITON FOR PLASMONIC WAVEGUIDE AND DEVICES

By
Salman Sadat Nur
12221104
Kashpia Zaman
16121047
Md. Ashaduzzaman Sarker
17121058
Abrar Zarif
17121029

A thesis submitted to the Department of Electrical and Electronic Engineering in partial fulfillment of the requirements for the degree of Bachelor of Science in Electrical and Electronic Engineering

Electrical and Electronic Engineering

Brac University

September 2020

Declaration

It is hereby declared that

1. The thesis submitted is my/our own original work while completing degree at Brac University.
2. The thesis does not contain material previously published or written by a third party, except where this is appropriately cited through full and accurate referencing.
3. The thesis does not contain material which has been accepted, or submitted, for any other degree or diploma at a university or other institution.
4. I/We have acknowledged all main sources of help.

Student's Full Name & Signature:

Salman Sadat Nur 12221104	Kashpia Zaman 16121047
Md. Ashaduzzaman Sarker 17121058	Abrar Zarif 17121029

Approval

The thesis/project titled “Graphene based surface plasmon polariton for plasmonic waveguide and devices.” Submitted by-

1. Salman Sadat Nur (12221104)
2. Kashpia Zaman (16121047)
3. Md. Ashaduzzaman Sarker (17121058)
4. Abrar Zarif (17121029)

Of Summer, 2020 has been accepted as satisfactory in partial fulfillment of the requirement for the degree of Bachelor of Science in Electrical and Electronic Engineering on 1st of October.

Examining Committee:

Supervisor:
(Member)

_____

Abu S.M. Mohsin, PhD.
Assistant Professor, Department of Electrical and Electronic Engineering
Brac University

Program Coordinator:
(Member)

_____

Abu S.M. Mohsin, PhD.
Assistant Professor, Department of Electrical and Electronic Engineering
Brac University

Departmental Head:
(Chair)

_____

Shahidul Islam Khan, PhD.
Professor and Chairperson, Department of Electrical and Electronic Engineering
Brac University

Abstract/Executive Summary

2D graphene was first discovered in 2004 and then it has gained admiration within scientific community due to its extraordinary electrical, mechanical, chemical and optical property. In this study, first we investigated the surface conductivity material model for graphene where we have found out that it is very much useful to characterize graphene modeling using a surface conductivity, which would help us to model graphene for other simulation. Then we demonstrated surface plasmon polarization for plasmonic waveguide and devices. Moreover, we showed optical absorption of a monolayer graphene and demonstrated maximum absorption rate of periodically patterned graphene. Then finally, using all these we designed an electro-optical modulator (EOM) and waveguides and devices based on graphene coated waveguide where we modulate the transmission and absorption rate of the modulator.

To do these experiments, we performed extensive numerical simulation using Lumerical FDTD, MODE, DEVICE solver based Lumerical software and verified the numerical results with available analytical analysis.

Keywords: graphene, surface plasmon, surface conductivity, waveguide, absorption, modulator, spp.

Dedication

DEDICATED TO OUR PARENTS AND OUR SUPERVISOR, DR. ABU S.M. MOHSIN, WHO PROPERLY GUIDED AND INSTRUCTED US TO COMPLETE OUR WORK IN TIME IN THE COVID-19 PANDEMIC SITUATION.

Acknowledgement

Firstly, we would like to convey our best gratitude to almighty Allah for His kindness and blessing. It would not have been possible for us to finish this thesis paper which we consider to be our one of the most important learning experiences of our undergraduate life without the praise of Allah.

Most importantly we are very grateful to our supervisor Dr. Abu S.M. Mohsin, Assistant Professor, Department of Electrical and Electronic Engineering, Brac University, for providing us a great opportunity to work with him in the arena of nanophotonic and nanotechnology. We are so lucky to get his tremendous support and proper guidance to finish our research in the time of global COVID-19 pandemic situation. Moreover, we would like to express our heartfelt appreciation to all the faculties and staffs of Electrical and Electronic Engineering Department of Brac University for their unconditional assistance in our hours of need.

Finally, we would like to thank our parents for always standing by us. It is their care, support and sacrifice that has encouraged us to come this far. We are very much thankful for everything they have done for us.

Table of contents

List of Figures

List of Tables

List of Acronyms

SPP	Surface Plasmon Polariton
FDTD	Finite Difference Time Domain
EOM	Electro-Optic Modulator
DOS	Density of states
EME	Eigenmode Expansion
FDE	Finite Difference Eigenmode
TM	Transverse magnetic waves
TE	Transverse electric waves
FDTD	Finite-difference time-domain

Chapter 1

Introduction

1.1 Introduction to graphene material

The idea of graphene was first introduced by the study of carbon fibers in Aerospace Industry. In this process, degree of graphitization was maintained by band position and intensity. In the year 2004, Graphene analysis hit the milestone as Geim and Novoselov introduced this unique 'Scotch Tape' method to insulate and designate graphene[1].

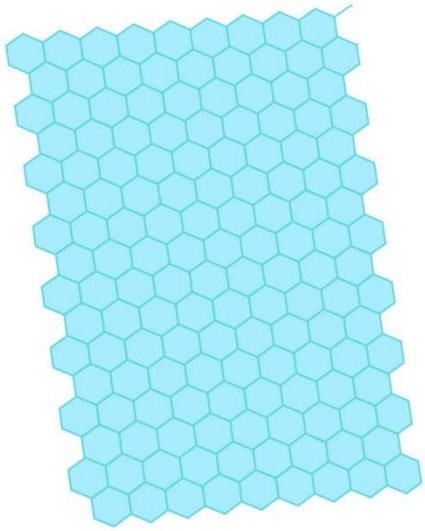

Figure 1: Single layer of 2D graphene sheet

Graphene can be specified as one of the incarnations of carbon which prevails in two-dimensional graphite (Figure 1)[2]. Monolayer graphite consists of carbon atoms which shares sp2 electron with their three adjacent carbon atoms[2]. After studying sp2 hybridization of the graphene, it can be seen that, 2pz orbitals form a plane π bond and planar

structure is perpendicular with it, along with molding a σ bond which is done by the sp2 hybridization of the orbitals[2]. As a result, we get a very strong σ bond which exhibits short interatomic with a length of 1.42 Aó and this quality makes it even more vital than the sp3 hybridized c-c bonds seems in diamonds[2]. This characteristic contributes to the astounding mechanical properties of graphene[2]. Studies show that, monolayer Graphene comprises of free-moving electrons on account of half-filled π band which is built by zero bang gap due between the conduction band and valence band[2]. Bilayer & multi-layer graphene are the outcomes of the π bonds that are responsible for the feeble Van-Der-Waals interconnection connecting the nearby Graphene layers[1, 3, 4].

1.2 Various properties of graphene material

1.2.1 Electrical properties of graphene

Graphene has many useful electrical properties. One of them is very high electrical conductivity[4]. Graphene is a zero-overlap semimetal material and it also has holes and electrons as charge carriers shown in Figure-2 [3, 4]. Carbon has 6 electrons in total where 2 electrons situated in the inner shell and 4 electrons situated in the outer shell[5]. Therefore, the outer shell electrons of carbon atoms are used for chemical bonding among other atoms[5]. On the other hand, in graphene atom there is a 2D plane where each carbon atoms is connected to another 3 carbon atoms[5]. So, for the electronic conduction in the third dimension 1 free electron is available which is called pi electrons[5]. Moreover, those pi electrons are located above the graphene sheet and below the graphene sheet and also intersect each other to improve the carbon to carbon bonds in the graphene [5-7]. Furthermore, the valance bands and conduction bands of these pi orbitals dictate the electronic properties of graphene[3, 7, 8]. Moreover, at the fermi dirac point the electrons and holes in graphene have zero effective mass because of its energy movement relation which is

linear for low energies near the 6 individual corners of the Brillouin zone which is known as dirac fermions and also for the 6 corners of the Brillouin zone which are known as the Dirac points[1, 3, 9].

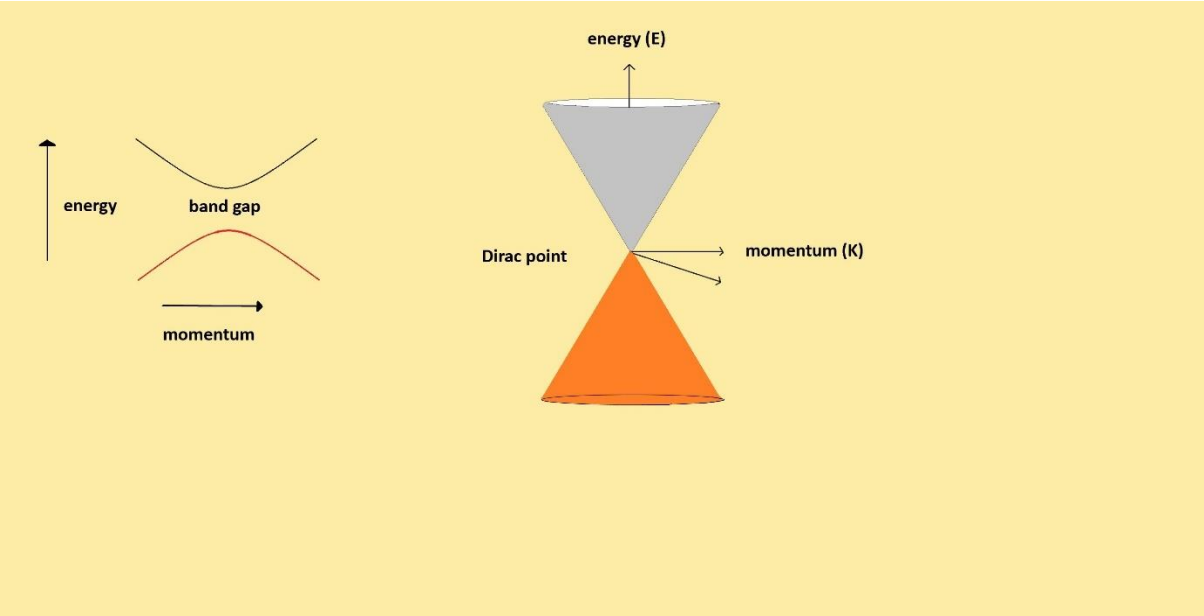

Figure 2: High electrical conductivity properties of graphene

At the Dirac fermion points the electric conductivity is also relatively low because of the zero density of states[9]. However, by doping with electrons or holes in the material fermi energy level can be changed to create a material which is possibly better at conducting electricity [3, 6, 7, 9].

1.2.2 Optical properties of graphene

Graphene have very high optical properties and it is capable of absorbing 2.3% of light constantly[4, 10]. Moreover, the uncommon low-energy electronic structure of monolayer graphene varies from quadratic huge bands which consists of electrons and holes conical bands at the dirac point (Figure 3) [7, 10, 11]. In past, many researchers and scientist showed how the amount of white light gets absorbed is depend on the strength of the electromagnetic collaboration between plain charged particles [11, 12]. However, if we add another layer of

graphene on it then it also increases the amount of lights get absorbed by the same value of 2.3% [13]. Graphene's optical absorption of 2.3% is always constant[13].

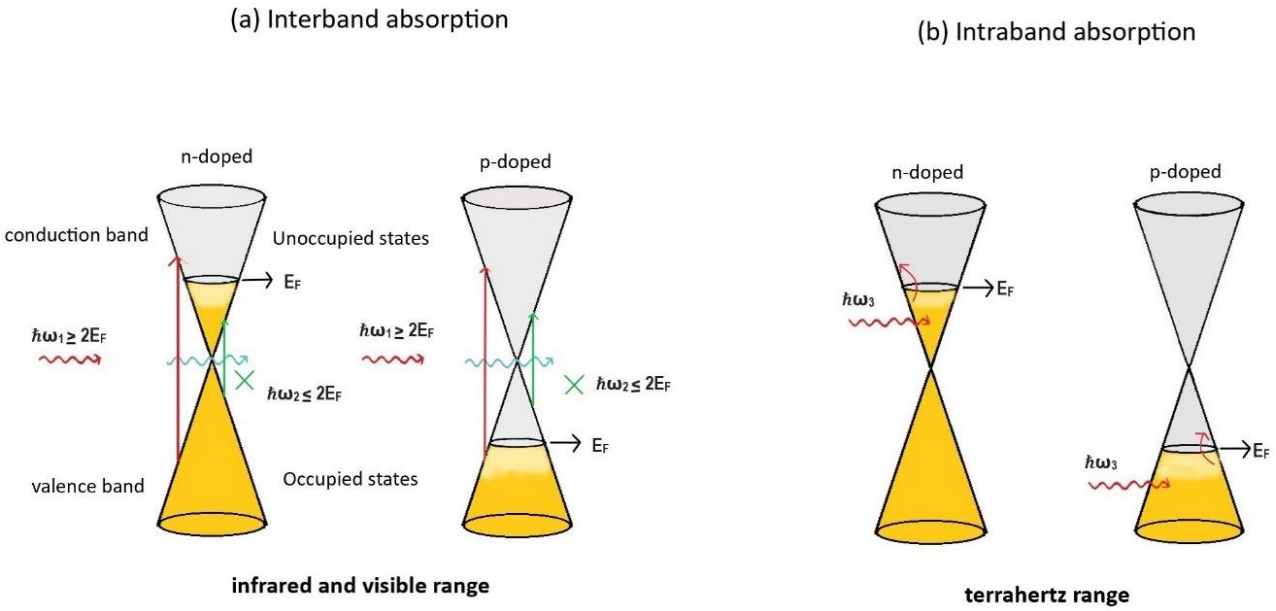

Figure 3: Very high optical absorption for (a)Interband and (b) Intraband for an atomic monolayer graphene.

Multi parametric surface plasmon resonance describes the thickness and refractive index of chemical vapor deposition which is grown in the graphene layers [4, 7, 11]. As we know saturable absorption is stated by non-linear optical behavior and the saturation fluence is known as threshold value. Therefore, because of the universal optical absorption rate of 2.3% and a zero band gap property of graphene, the strong excitation over the visible to near-infrared region is capable of saturating graphene readily[7, 11, 14]. As graphene based saturable absorber is used for full band mode locking, it has contributed to its massive approach in the ultrafast photonics applications [11, 14]. Moreover, we can tune the optical response of graphene layers electrically [11, 14].

1.2.3 Mechanical properties of graphene

Graphene's another amazing property is its intrinsic strength. Graphene is called the strongest material ever discovered due to the carbon bonds strength of 0.142 Nm-long, which also have an intrinsic tensile strength of 130 Gpa (19000000 psi)[4]. For stretching graphene's large part freestanding, the equivalent representative engineering tensile strength is about 50-60 gpa and there is also a Young's Modulus which is close to 1 Tpa (150000000 psi) [4, 7].

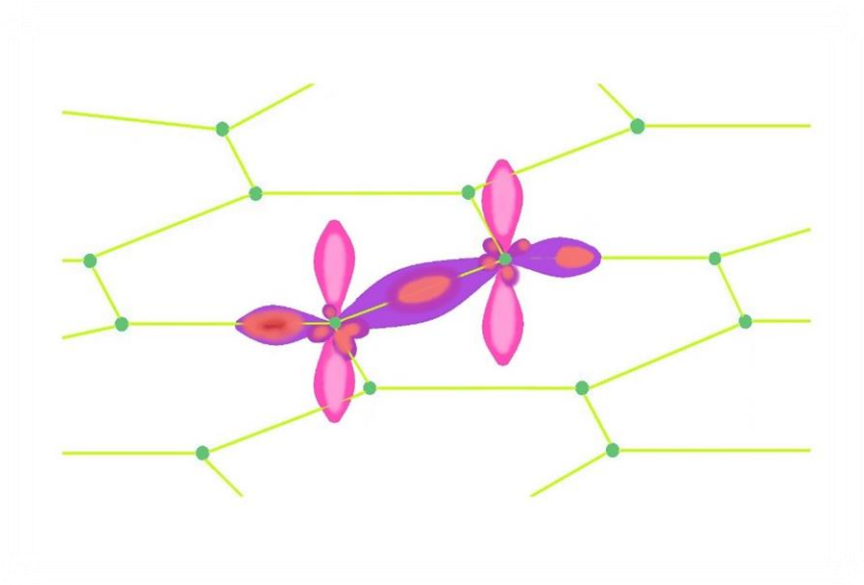

Figure 4: Graphene's carbon bonds strength.

Therefore, large angle bent Graphene monolayer can be accomplished with very little strain which also exhibits mechanical robustness of the 2D-Carbon nanostructure(Figure 4) [7]. However, Graphene monolayer also has excellent carrier mobility despite of its extreme deformation[1, 7, 15].

1.3 Various applications of graphene:

Graphene has a huge number of applications in mechanical Engineering, electrical engineering, micro-electronics, biomedical industry and therefore it is considered to be the most important material in electronics engineering as a elemental material[4].

Being the world's strongest material, graphene can be used to strengthen other material. Researchers prove that adding even the slightest amount of graphene to plastics, metals or other material can efficiently make these material much effective and powerful as well as lighter[7].

Graphene being the most heat conductive, strong and light, it is heavily used for making heat-spreading solutions, such as heat sinks or head dissipation films[1, 3, 7]. Microelectronics (For example, to make LED lighting more efficient and long-lasting) and in larger applications such as thermal foils for mobile devices. Graphene based thermal films are used in Huawei's latest smartphones[7].

As Graphene has high surface area to volume ratio owing to it's being the world's thinnest material, Graphene has introduced revolutionary uses in batteries and supercapacitors[7]. Graphene can permit batteries, supercapacitors and even fuel cells to store more energy and charge faster.

Graphene also have some groundbreaking applications in anti-corrosion coatings and paints, flexible displays, sensors, solar panels, faster and efficient electronics, faster DNA sequencing and many more[3, 16]. In 2017, MIT researchers were able to use graphene successfully on a solar cell. Studies have proven that Graphene solar cell was as good as the ITO cell and not as good as Al if considered current densities and power conversion efficiencies[11].

Graphene is used in Li-ion batteries that exhibits longer lifespan, higher capacity and faster charging time as well as flexibility and lightness, to make it usable for wearable electronics[1, 3, 7].

1.4 Surface Plasmon polariton (SPP) of graphene

Graphene has a very linear distribution relation and other the extraordinary fermions properties[17]. It is mainly a two-dimensional monolayer of carbon atoms arrayed in a honeycomb lattice structure with a promising electronic and photonic applications [1, 3, 17]. The infrared or visible frequency generated from the electromagnetic waves and a metal dielectric or metal-air interface when interact the electron density wave involves charge ratio which propagates along the surface of the metal is known as surface plasmon polariton (Figure 5) [18].

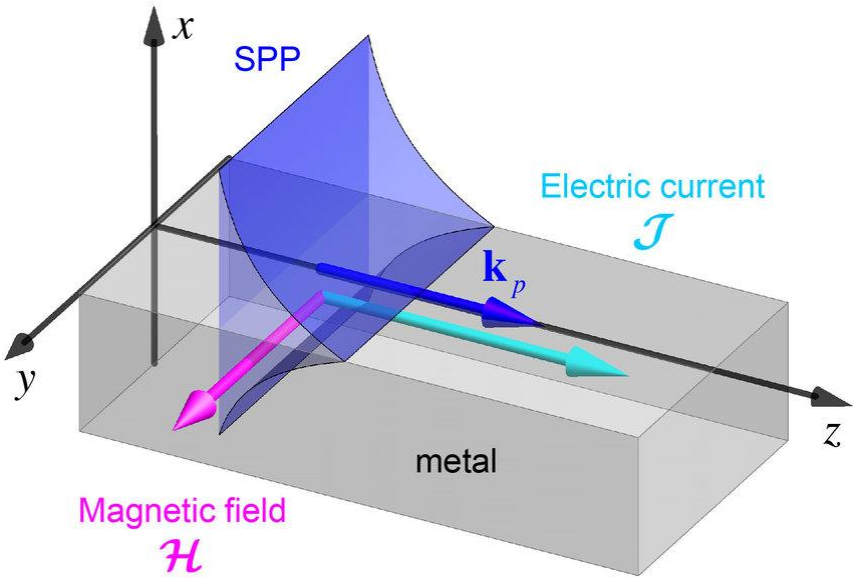

Figure 5: Schematic of a surface plasmon polariton (SPP) propagating along the metal vacuum.[19]

In plasmonic graphene surface plasmons excitations are much more restricted than orthodox noble metals[17]. Here the electron oscillations and electromagnetic field interacts[18]. Moreover, graphene has a very flexible nature and very little transmission loss property which makes it a very potential material for plasmonic field applications [17, 18].

1.5 Plasmonic waveguide of graphene

Graphene a has the optical properties of surface plasmon polariton (SPP). When the graphene SPP occurs at a metal–dielectric interface where another new group of waveguides made of insulating and conducting materials generates[20, 21]. This kind of novel waveguides which generates from such conditions are known as plasmonic waveguides or SPP waveguides of graphene[20].

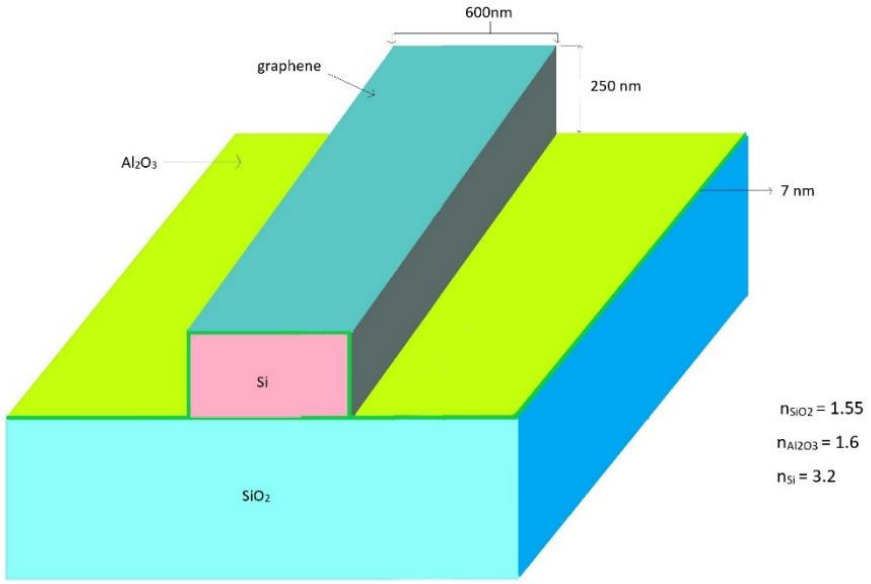

Figure 6: An electro-optical modulator using Si waveguide core.

However, those dielectric waveguides guide are light by using the index of refraction difference between the layer and core media of the structure[20]. Moreover, some SPP waveguides guide wave modes at the interface between a metal surface and a dielectric medium in a structure [4, 20]. Thus, the permittivity of the constituted media always has opposite signs. One in every of the foremost advantages of plasmonic waveguides is that the wave energy can confined within a tiny low spatial cavity[20]. Plasmonic waveguides have the ability to guide the long or short range of SPP waves[20]. We determine the structure and transverse core dimensions depending on the working condition. However, the graphene-

based waveguides are divided into rectangular and cylindrical waveguides[20]. In both categorizes, either graphene biased in electrically or it is simultaneously biased in magnetically and electrically where the conductivity of graphene becomes a tensor[20].

1.6 Motivation

Graphene is a very promising and useful material in the modern science and industrial sector. As only in 2004, it was physically possible to isolate a graphene layer from graphite. From that time, various researches are done to find its characteristics and application in the real world. In the previous researches, we find out many of the graphene's unique properties. It has unique mechanical, optical, electrical and chemical properties. It is almost 300 times stronger than metal, but very light in weight. It is stronger than diamond and can carry current without any resistance. On the other hand, diamond can't carry current effectively at all but graphene's electric conductivity is very high. So, it can work as a very good conductor. From its mechanical properties we know that graphene's dimension, structure, shape can be tuned and it can be used for coupling. Graphene also can be used as a waveguide material. Moreover, graphene can be used as a low-cost photo detector. In the market, most of the current photo detector devices used in remote devices, sensors and in light-based communications are very expensive. But graphene-based photo detector device can lower the cost significantly. Graphene hybrid solar cells also has a great potential in Photo voltaic sector, as it is less expensive than pure silicon based solar cells and shows near performance of silicon cells.

Yet, majority of the characteristics and application of the graphene are not being used extensively as it is still too new and technologies for processing and patterning it are still in relatively early stages of development. By studying graphene's properties and doing some researches, here we would like to work on the surface plasmon polariton for plasmonic

waveguide and devices based on graphene. Therefore, in real life we can improve its understandings and apply in different fields of our daily life.

1.7 Aims and Methodology of the Thesis

In this section, we discuss the specific aims of this thesis, potential research problems and proposed techniques to achieve our intended goals.

At first, we want to develop an efficient model by developing a surface conductivity model of graphene layers. We also want to observe the surface plasmon polariton effect for graphene based plasmonic waveguides. Then would like to demonstrate the 100% optical absorption rate in periodically patterned graphene. And finally using those studies, we would like to develop an elctro-optical modulator based on graphene coated waveguide where we will try to achieve the optical absorption by tuning fermi energy level of graphene.

In order to achieve our desired results, we use a clear methodology. We approached this methodology by developing analytical studies and also numerical studies. For numerical studies we use Lumerical FDTD, MODE and DEVICE solution software. Then we will compare the numerical results with our analytical results.

1.8 Thesis Structure:

Our thesis work has been categorized into different chapters. Each chapter principally focused on a particular part to achieve precisely the goals of our research. To begin with, in chapter 1 we mainly focus on Graphene's different properties, spp, waveguide and the wide range of applications. Chapter 2 demonstrated the modeling approach using surface conductivity material model of graphene, where we showed the theoretical approach to calculate the surface conductivity of graphene. Chapter 3 explained the TM and TE surface plasmon polariton of graphene and the transmitted. Chapter 4 covered the optical absorption

rate of graphene and experimentally shows the 100% absorption for a periodically patterned Graphene. Chapter 5 demonstrate an electro-optical modulator which is mainly based on graphene and we try to improve the absorption and transmission of the modulator by changing the fermi energy level and chemical potential of graphene layer. Chapter 6 concluded the study of the thesis including a description of our significant achievements along with our future work plan.

Chapter 2

Graphene modeling approach

2.1 Introduction

Graphene is a very thin carbon atom and a single layer material with a thickness of one atom. Therefore, it is usually characterized by surface conductivity material model instead of using a volumetric permittivity material model, which makes graphene different from other optical materials. In this chapter we will demonstrate the graphene material model in FDTD using surface conductivity model

2.2 Introduction to the graphene surface conductivity material model

Graphene have some great optical properties. Normal carbon atom has 6 electrons, 2 in S and 4 in P shell. Those 4 electrons are used for chemical bonding with other atoms[12]. Thus graphene stay in 2D dimension, so each atom of graphene is connected with another 3 carbon atoms on the 2D plane and leave 1 free electron[12]. This free electro is called pi electron and it is located above or below the 2D graphene sheet. This Pi electron gives excellent Electric surface conductivity to the Graphene[3, 22]. Graphene is a different material from most of optical materials which has a very thin one atom thickness material layer[23]. Therefore, using any material model we can combine graphene layers into optical simulations[23]. However, volumetric permittivity needs very fine discretized grids, so that is not very efficient model[23]. Therefore, researchers and scientist found a more efficient by using Maxwell's equations in the time or frequency domains[23]. There they incorporate a surface conductivity material model description of graphene layers with a volumetric permittivity material model description and resolved the problem [23]. Therefore, in this chapter we are going to review graphene's surface conductivity model material. Then we will try to simulate

this in Lumerical FDTD simulation and try to observe the corresponding surface conductivity with our analytical result.

2.3 Literature review of graphene surface conductivity material model

As we know, Graphene is a relatively new material in the field of Electrical conductivity. There is huge potential about graphene and lots of research are taking place. Thus, we are also trying to find its hidden potentials. At present, we are using Copper as an ideal conductivity material. But it is both expensive and rare. So, we are using Graphene as an alternative because Graphene is considered as an ideal substitute for replacing Copper. For the better and elaborate understanding the Graphene's conductance, we need to know the surface conductivity of Graphene material.

As we know graphene is a very small and thin material with a thickness as small as one atom size [3, 24]. So, most of the time it is usually defined and characterized for many applications by using a surface conductivity material model[5]. Here, we have discussed the theory of calculating surface conductivity of graphene layer and then we demonstrate it in the experimental simulation setup [25, 26].

For a single layer of graphene surface conductivity is calculated by[5],

$$\sigma(\omega, \Gamma, \mu_c, T)\& = \sigma_{\text{Intra}}(\omega, \Gamma, \mu_c, T) + \sigma_{\text{Inter}}(\omega, \Gamma, \mu_c, T)$$

Where the symbols represent,

ω = Angular frequency,

Γ = Scattering rate,

μc = Chemical potential,

T = Temperature,

e = Electron charge,

$\hbar$ = Reduced Plank constant,

kb = Boltzmann constant.

We also need to calculate the inter band and intra band surface conductivity of graphene. To do so the Inter band surface conductivity is calculated by,

$$\sigma_{\text{Intra}}(\omega, \Gamma, \mu_c, T) = \&\frac{-ie^2}{\pi \text{H}^2(\omega + i2\Gamma)} \int_0^\infty \xi \left(\frac{\partial f_d(\xi)}{\partial \xi} - \frac{\partial f_d(-\xi)}{\partial \xi} \right) d\xi$$

And the Intra band surface conductivity is calculated by,

$$\sigma_{\text{Inter}}(\omega, \Gamma, \mu_c, T)\& = \frac{ie^2(\omega + i2\Gamma)}{\pi \text{H}^2} \int_0^\infty \frac{f_d(-\xi) - f_d(\xi)}{(\omega + i2\Gamma)^2 - 4(\xi/\hbar)^2} d\xi$$

We also calculated the Fermi-Dirac distribution by using,

$$f_d(\xi) \equiv \frac{1}{\exp((\xi - \mu_c)/(k_B T)) + 1}$$

And finally we get the intra band conductivity of graphene layer by using the formula,

$$\sigma_{intra}(\omega, \Gamma, \mu_c, T) = \frac{ie^2 k_B T}{\pi \text{H}^2(\omega + i2\Gamma)} \left[\frac{\mu_c}{k_B T} + 2\ln\left(\text{Exp}\left(-\frac{\mu_c}{k_B T} \right) + 1 \right) \right]$$

After calculating the surface conductivity of graphene analytically, we therefore use an experiment to compare our results.

2.4 Simulation setup process

We use Lumerical FDTD solution for our simulation setup, where we set a 2D rectangular Graphene material. In our experimental setup in FDTD we have used the scattering rate value

of 0.41 meV, then chemical potential value of 0.2 eV, then the temperature value of 300k and also use scaling factors value of 1 for better results[22, 23].

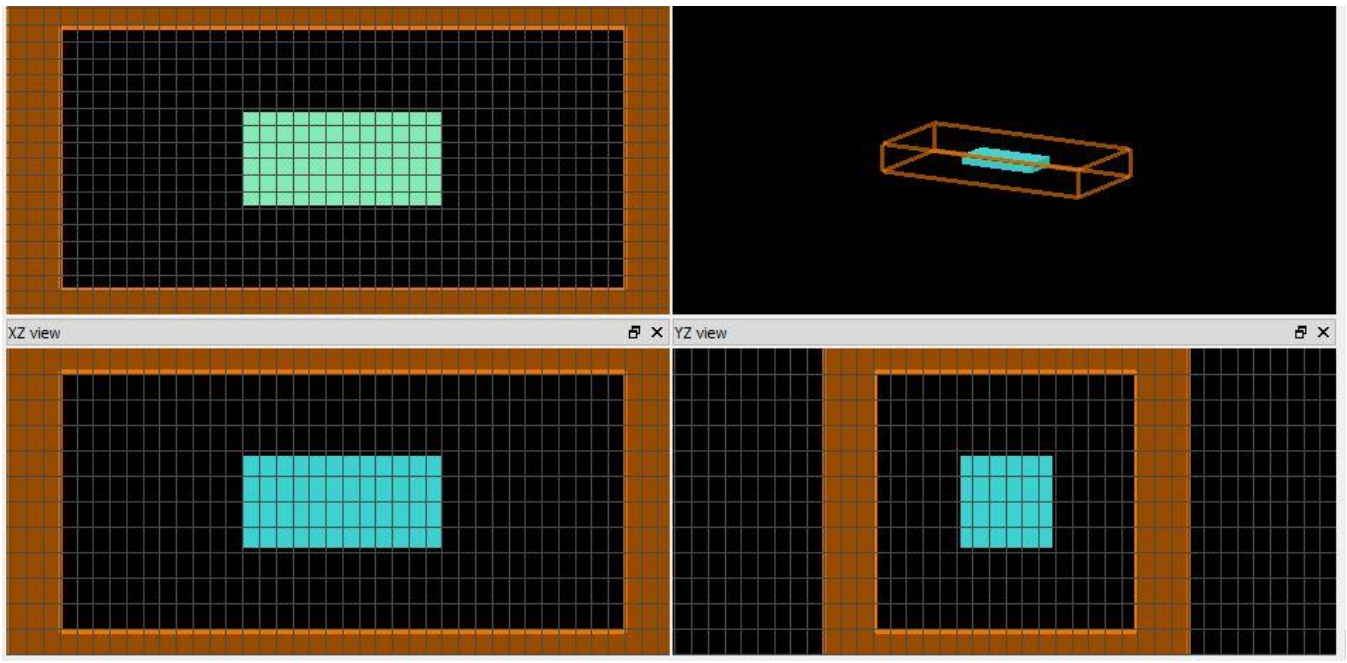

Figure 7: Lumerical FDTD simulation setup for Surface Conductivity Calculation.

According to those factors, we get the corresponding interband surface conductivity material model for a flat surface. Then, we get the surface conductivity graph from our simulation.

2.5 Results and discussion

We calculate intra band conductivity of Graphene layer analytically and the inter band conductivity numerically from our simulation setup. We get two graphs for surface conductivity real part and imaginary part with respect to frequency. From the graph (Figure 8) we can observe that in both real and imaginary part the numerical data is same with the analytical data.

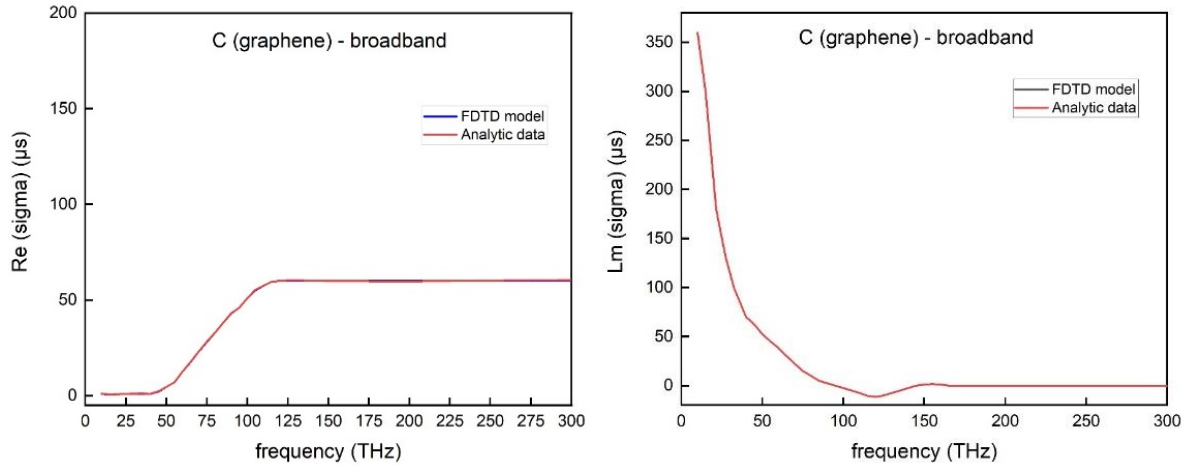

Figure 8: Real part (Left) and imaginary part (Right) of the surface conductivity model of graphene layer where the analytical data and experimental data match each other[23].

Therefore, we can say that graphene can be characterized by using a surface conductivity material model instead of using a volumetric permittivity material model as our analytical values are similar compared to the experimental FDTD data showed in Figure-8[5].

2.6 Conclusion

We try to demonstrate the surface conductivity material model of graphene layer by using analytical and numerical methods. We calculate intra-band conductivity analytically and inter-band conductivity in Lumerical FDTD. We are able to plot real and imaginary surface conductivity graph. We find that, numerical data is match with analytical data which shows that, graphene has high surface conductivity. This graphene surface conductivity material model will allow 2D graphene to be accurately simulated without keeping the mesh size small and will also help to get results much quickly.

Chapter 3

Exciting surface plasmon waveguides of graphene

3.1 Introduction

In this chapter we demonstrate the surface plasmon-polaritons on graphene based crystal structure and observe the spp in their plasmonic waveguides of graphene using Lumerical FDTD software. For that reason, first we discuss the different structure for calculating spp in plasmonic waveguides. We also try to find the best substrate material to use in the structure to get better surface plasmon polaritons for different materials.

3.2 Different structure model for exciting and detecting surface plasmon polariton.

To observe the spp in a graphene-based surface plasmon waveguide structure we use TM and TE surface plasmon polarized modes to excite them. To model those structure here we use two common approaches otto configuration and Kretschmann configuration.

3.2.1 Otto configuration

We use otto configuration in p-polarized TM surface plasmon. When a graphene layer is placed on the top of a substrate or multilayer structure (Figure 9) and the photonic light gets attached through a prism situated on top of the whole structure is known as otto configuration [23]. Moreover, there is a small distance between the metal surface and the TIR surface of the structure[27]. The gap is filled with a very lower refractive index medium to overcome problems (Figure 9)[23, 27].

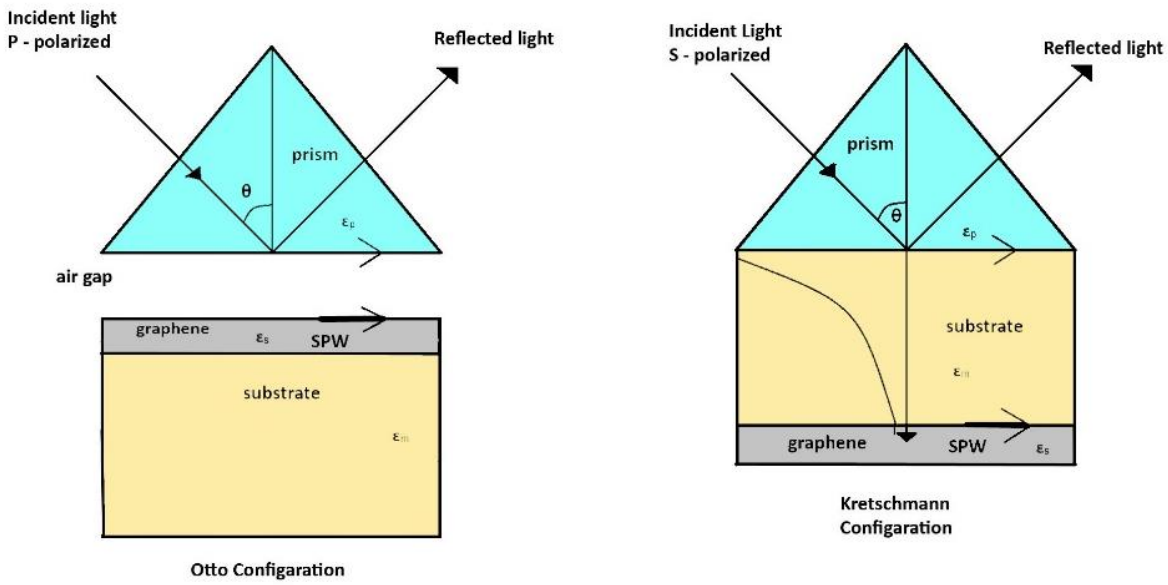

Figure 9: Otto configuration(left) and Kretschmann configuration (right)

3.2.2 Kretschmann configuration:

We use kretschmann configuration in s-polarized TE surface plasmon. When a graphene is placed on top of a substrate or multilayer structure and then the photonic light is being coupled through a prism below the structure[23]. This whole phenomena is known as kretschmann configuration (Figure 13*)* [23].In kretschmann configuration the metal layer of the structure stays on the top of the TIR surface of the structure and it helps to enable more efficient spp generation [23, 27].

3.3 Exciting a S-polarized (TE) surface plasmon on graphene

3.3.1 Introduction

In this experiment, we are trying to establish a design consists of a supporting crystal structure which will help us for getting the excitation values of our experimental setup and comparing results with the analytically projected TE polarized excitation in a single graphene sheet[28]. We explain the way we measure the excitation at room temperature. We also

observe the transmitted and reflected power and the electric field profile with respect to the source angle and also compare those experimental results with the analytical results[4].

3.3.2 Literature review

As we know, when we couple between the source and TE mode, it becomes very strong when the projection of the source wave vector of the plane wave matches the corresponding components of the surface plasmon's wave vector[28-30]. This can be done by fixing the angle of incidence of the source. For that reason, we need to calculate the surface Plasmon mode. In our experiment we use 2D graphene sheet and its conductivity is,

$$\Sigma=(15.98-i27.69)\ \mu s \quad (\text{At near-infrared} 1.31\ \mu m).$$

For calculating angle of incidence of the source, we know here,

$$N_{eff}=1.116+i0.002$$

Now, the angle of incidence of the source is,

$$\boldsymbol{\Theta_{sp}} = \arcsin(\mathrm{Re}(n_{eff})/n_{glass}) = 50.5 \text{ deg} , (\text{where, } n_{glass} = 1.98)$$

So the excitation of surface Plasmon is strongest around the source angle of 50.5 degree[28]. We observe the reflected and transmitted power with respect to the source angle ($\boldsymbol{\theta_{sp}}$**).** Moreover, we show the electric field intensity with respect to source angle ($\boldsymbol{\theta_{sp}}$).

However, When the waves generated from source in one medium then it reaches the boundary of another medium at a sufficiently slanting angle. Therefore, the second medium become transparent to the waves and allows them to travel more faster, which creates Total Internal Reflection (TIR). We know that, angle of incidence of the source is always greater than the angle due to total internal reflection ($\boldsymbol{\theta_{sp} > \theta_{tir}}$**)**[28].

3.3.3 Simulation setup process

In this 2D FDTD experiment setup (Figure 10), we place a TE (S-Polarized) surface Plasmon on a graphene layer above the photonic crystal[30]. Under that, we use TiO_2 layers and SiO_2 layers. The surface plasmon of the mode is excited by a plane wave source which is situated inside the glass substrate according to the Kretschmann configuration as described before[30]. We also set PML boundary condition along X axis and Bloch boundary condition along Y axis. In graphene layer, we use graphene as material in 2D geometry shape.

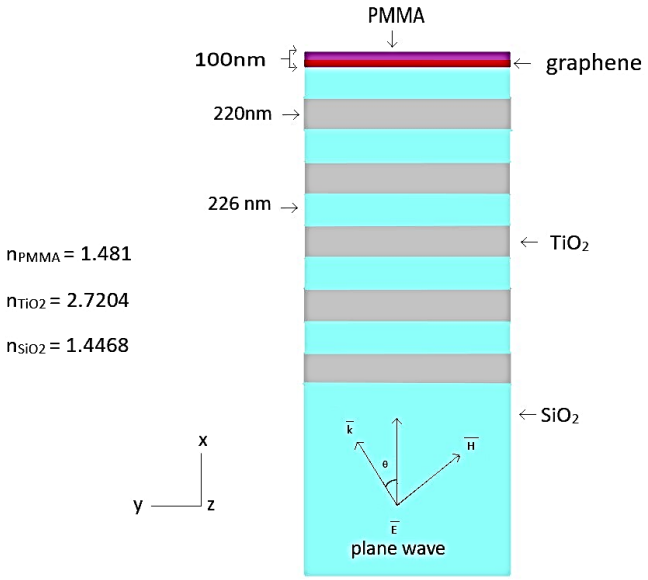

Figure 10: Structure of a TE (s-polarized) surface plasmon using Kretschmann configuration[23, 30].

We also use two monitors to observer the transmitted and reflected power at different source angle. A time monitor is set up to get real time simulation result. Across the simulation region for observing the field profile we set up a field monitor.

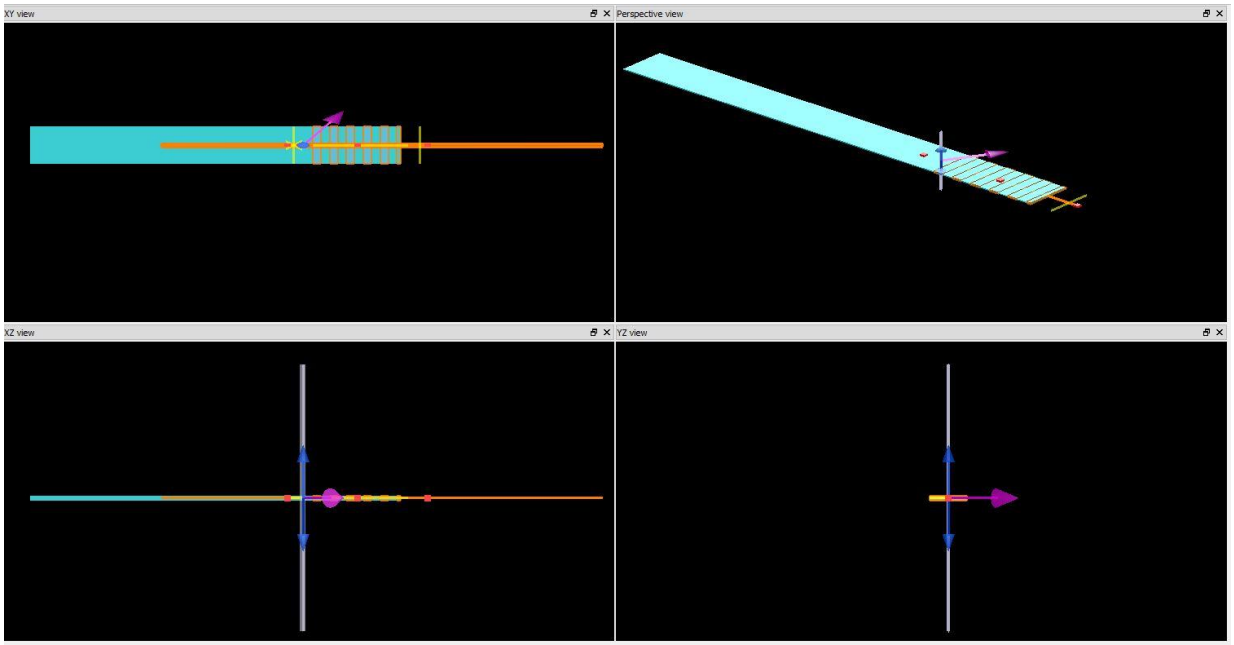

Figure 11: Simulation setup in Lumerical FDTD for exciting as-polarized surface Plasmon on Graphene.

3.3.4 Results and discussion

We open the FDTD file in lumerical software and then run the script for getting the transmitted and reflected power for source angle in between 43 and 60.

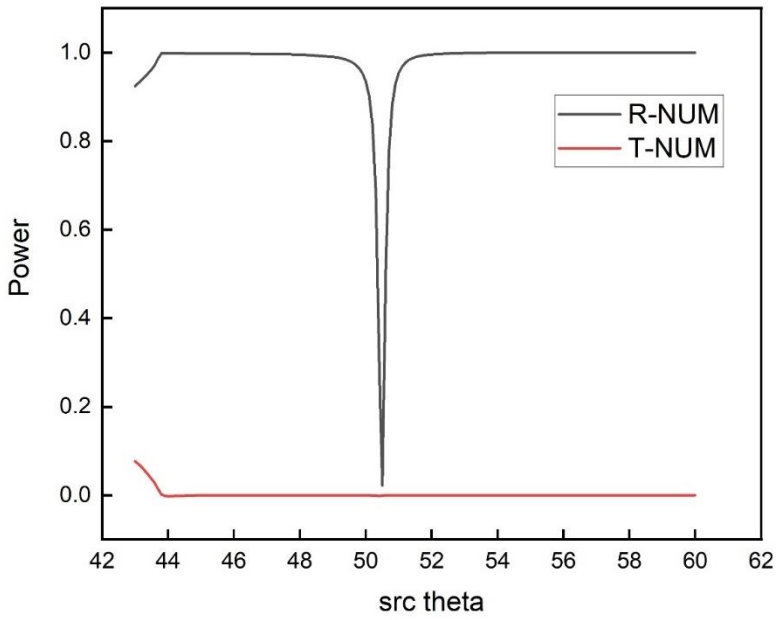

Figure 12: Plot of the numerical values of the reflected and transmitted power with respect to source angle where spp visible at 50.5 degree.

After observing the graph (Figure 12), we see that the experiment values match the analytical values. However, we can see a dip in the reflected power occurs at the source angle $\boldsymbol{\theta_{sp}}$ 50.5 degree. This dip happens because the photonic crystal region fields are purely evanescent[23]. As the evanescent field excites the surface plasmon of the graphene, the reflected power decrease exponentially with the increase of source angle which create such a dip in the reflected power. We can also see that, source angle angle $\boldsymbol{\theta_{sp}}$ is greater than the angle due to TIR (Total Internal Reflection) ,($\boldsymbol{\theta > \theta_{tir}}$)[21, 28, 31].

However, we also run FDTD to see the electric field intensity generated in the simulation region for the source angle values between 43 and 60 degrees[31].

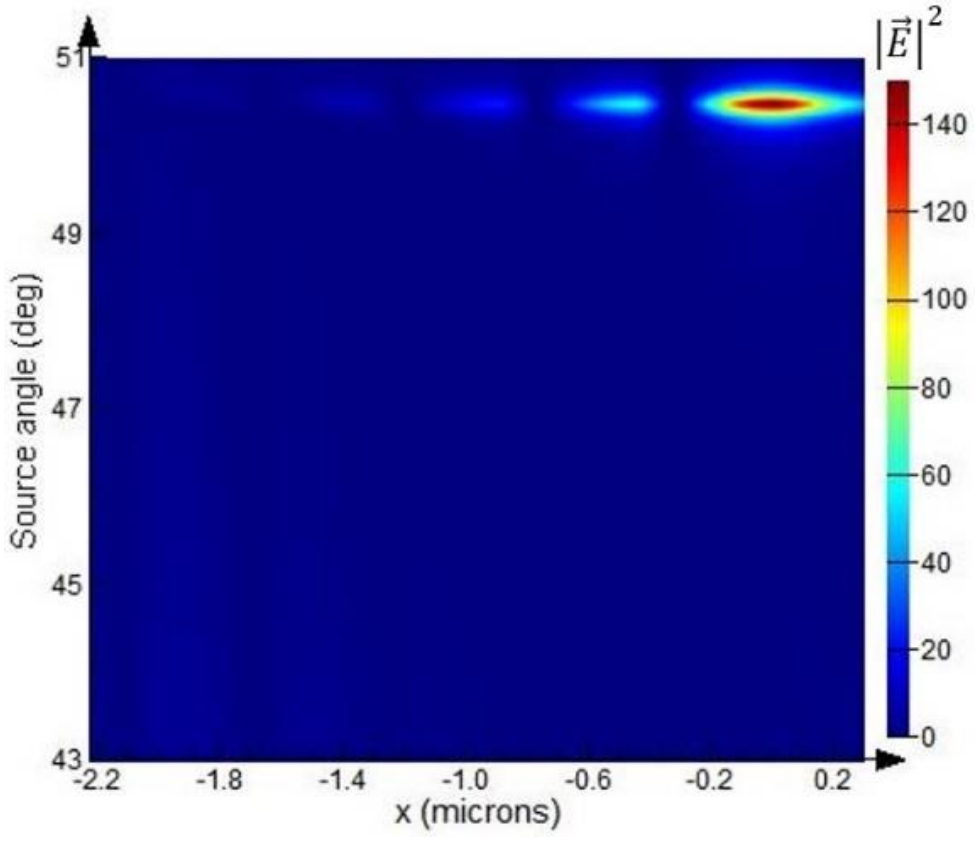

Figure 13: Electric field intensity along x direction with respect to source angle 50.5 degree.

We can see (Figure 13) the concentration of electric field intensity is also high at source angle 50.5 degree along X axes. Therefore, we can say at source angle 50.5 degree excitation is strongest and also electric field intensity is very high[23].

3.4 Exciting a p-polarized (TM) surface plasmon on graphene

3.4.1 Introduction

This experiment shows the effectiveness of using FDTD when we try to simulate any graphene-based devices where we will excite a P-polarized surface plasmon consist of a graphene layer on top of a glass substrate[4]. And we will also try to show using Silicon substrate and Titanium substrate instead of glass. We find the best way to excite the p polarized surface plasmon. These results will help us to compare the analytical results with our simulated numerical results of transmitted and reflected power and also let us know the spp effect on the graphene[4].

3.4.2 Literature Review

When we excite a p-polarized (TM) surface plasmon in graphene, then the excitation of the wave vector is much stronger at times when the propagation of the plane sources wave vector onto the prism air boundary is same as the corresponding components of the surface plasmons wave vector[30, 32, 33]. For that reason, we compare the reflected and transmitted power and also electric field intensity at source incident angle.

In our experimental setup, the effective index of surface plasmon,

$$n_{eff} = 2.56 + i0.12$$

From that we can measure the incident angle of the surface plasmon.

Optical coupling angle or source incident angle for the plane wave is,

$$\theta_{SP} = \arcsin\left(\mathrm{Re}\left(n_{eff}\right)/n_{prism}\right) \approx 30.8^{\circ}$$

As we use prism surface and it's refractive index n_{prism}=5 and glass as substrate for which refractive index n_{glass}=1.98. Therefore, around 30.8° surface plasmon mode excitation is strongest on the graphene surface[23, 34, 35].

When waves in one medium reach the boundary with another medium at a sufficiently slanting angle, therefore the second (external) medium is transparent to the waves and allows them to travel faster than in the first (internal) medium is known as Total Internal Reflection (TIR)[23, 35, 36]. In our experiment, Total internal reflection (TIR) occurs but the source angle due to the surface plasmon must be always bigger than the angle of the total internal reflection($\theta_{sp}>\theta_{tir}$)[31]. Therefore, we observe the simulation graph to know θ_{sp} and θ_{tir} relationship.

3.4.3 Simulation Setup Process

We use the Lumerical FDTD simulation setup in an Otto configuration (Figure 14) to match our experimental results with the analytical results. In our simulation setup we use a plane

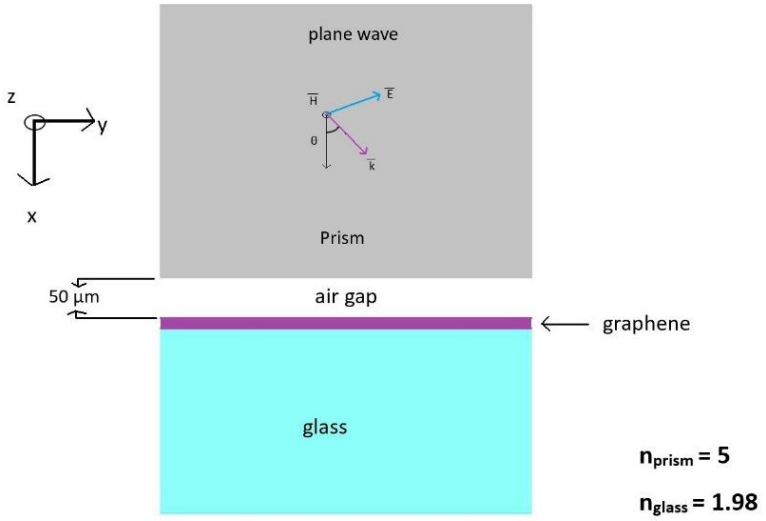

Figure 14: Experimental setup for the p-polarized TM surface plasmon using Otto configuration.

wave source on a prism surface which has very high refractive index ($n_{prism=}5$). The prism surface is separated from grapheme layer by a small airgap (50 µm). The graphene 2D layer is deposited on a glass substrate[23].

We also use a time monitor to get time-domain information for the field components of the simulation[37]. Moreover, we add a field monitor to collect the field profile in the frequency domain from numerical simulation results across the simulation region[37]. Furthermore, we set a front mirror and a back mirror to collect the data of reflected and transmitted power and also for electric field intensity values.

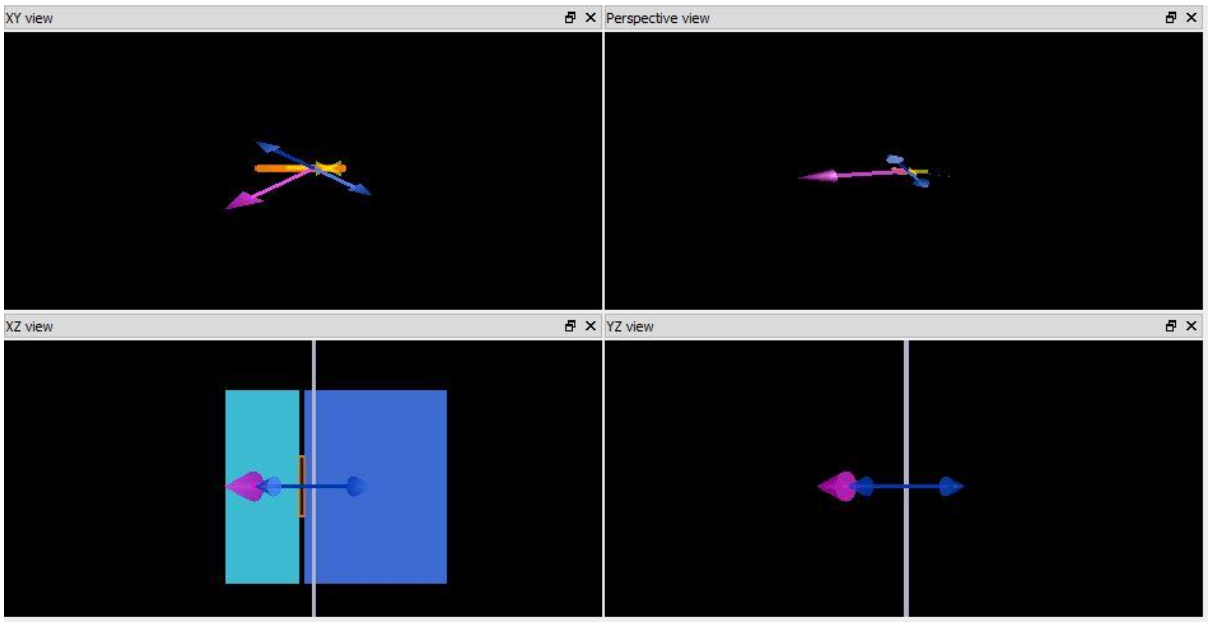

Figure 15: Simulation setup in Lumerical FDTD for exciting a p-polarized surface Plasmon on Graphene.

We set the mesh accuracy 4 and PML layer 24 to get better results similar to the theory. First we simulate the setup using glass substrate and then we substitute the glass substrate with Silicon and Titanium accordingly and observe the results among them.

3.4.4 Results and discussion

Using Glass substrate:

To get the results from our simulation setup we construct our Lumerical FDTD setup in Lumerical Inc software and Then we run the script for incident angle from 5°- 45° and get the reflected and transmitted power for the incident source angle.

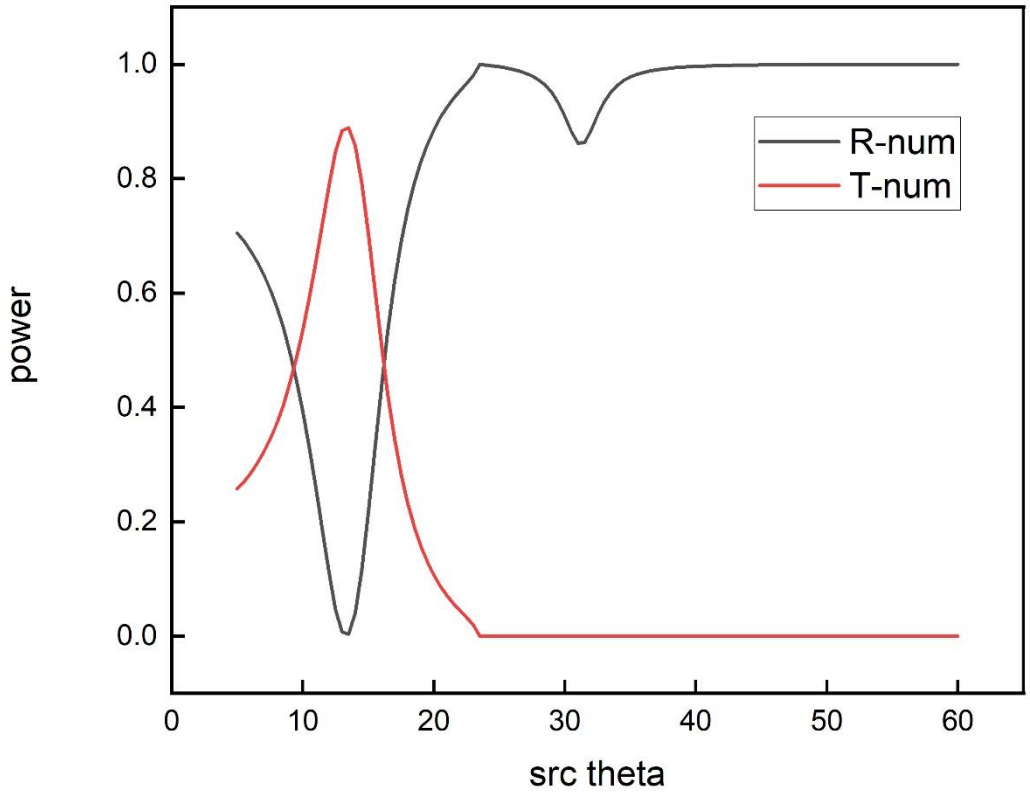

Figure 16: The simulated reflection and transmission power with respect to source angle using glass substrate where spp is around 32 degree[38].

For the graph (Figure-16), we see the Total Internal Reflection (TIR) is greater than 23° and the surface plasmon mode is around 32°. Therefore, the angle due to surface plasmon (θ_{sp}) is bigger than the angle due to total internal reflection (θ_{tir})[31]. As the airgap is momentary

here, so the fields should be reflected. However, we can see a dip in the reflection power which happens at source angle (θ_{sp}), which is opposite to the total internal reflection (TIR) of the mode. The evanescent field excites the surface plasmon of the graphene sheet and therefore there is a deep in the reflected power. Therefore, the amplitude of the reflected power decreases exponentially with the increasing source angle[39]. This evanescent field creates such reflection drop in the graph[23].

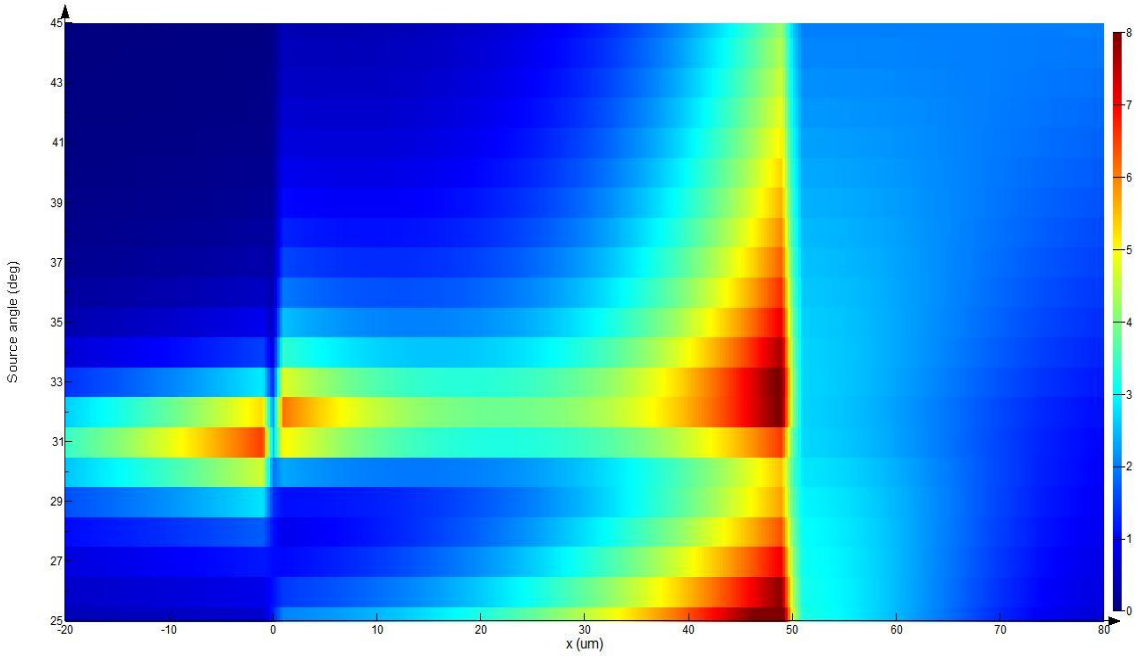

Figure 17: The electric field intensity corresponds to Source angle using Glass substrate.

Moreover, we also measured the electric field intensity for the source angle 25°-45°. In the graph (Figure-17) we can see the surface plasmon mode is visible around $\theta_{sp.}$, where the electric field intensity is very high.

Using Si substrate:

We use silicon substrate instead of glass which has refractive index of 3.9766. We ran simulation setup in FDTD and run the script for source angle 5°-45° to get reflected and

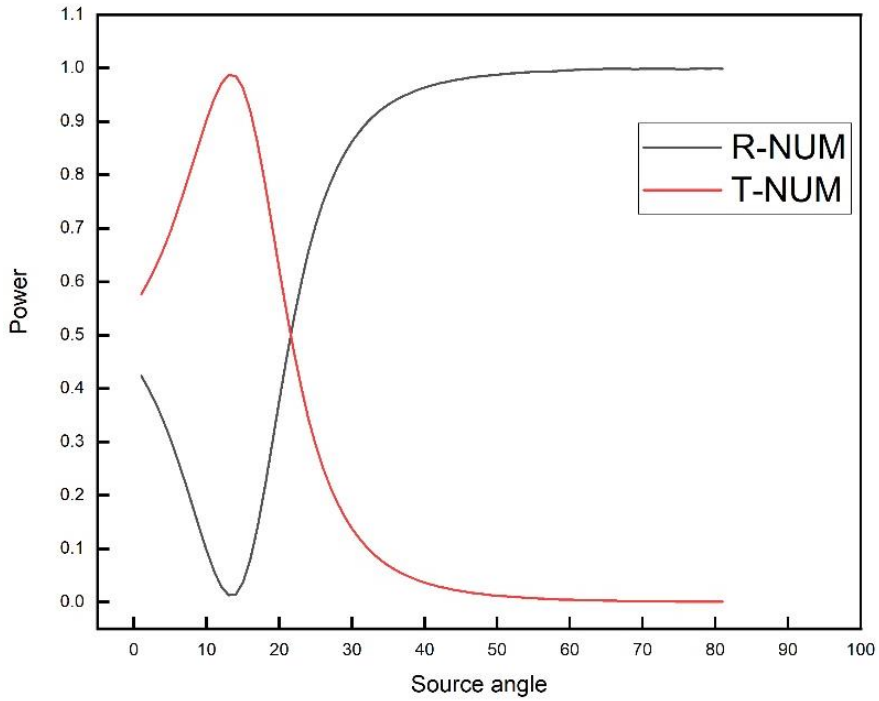

Figure 18: The plot of reflected and transmitted values as a function of source angle using Si substrate.

transmitted power versus source angle graph (Figure 18) and also for source angle 25°-45° to get a graph for electric field intensity versus source angle (Figure 19).

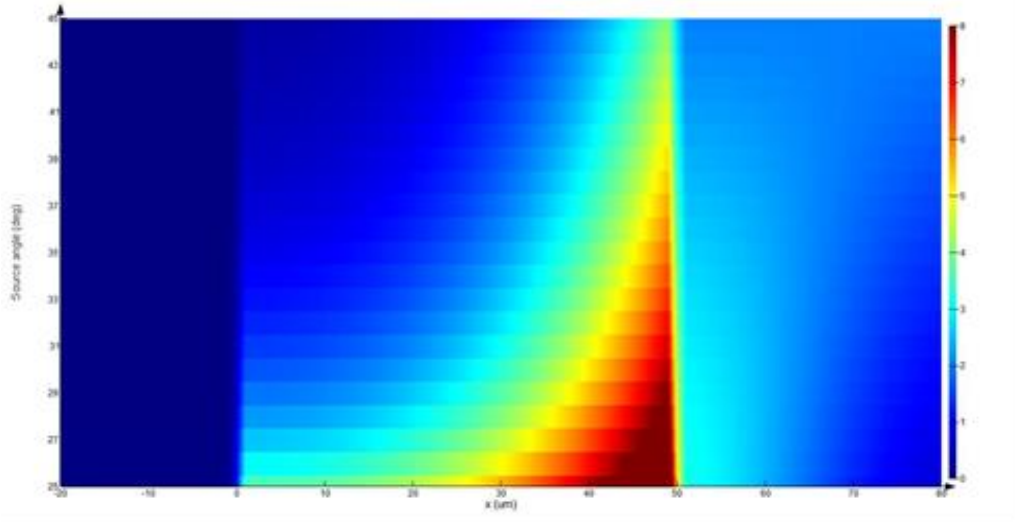

Figure 19: The electric field intensity with respect to source angle using Si substrate.

From the graph (Figure 18), we can see that it doesn't match our analytical results. In the reflected power there should be a dip at source (θ_{sp}) because of evanescent field effect. On another graph (Figure 19) the electric field intensity for (θ_{sp}) is much lower which is not desired. Electric field intensity must be strongest at $\theta_{sp.}$

Using Ti substrate:

We set Ti substrate instead of glass and refractive index of Titanium is 2.6112. We ran simulation setup in FDTD and run the script for source angle 5°-45° to get reflected and transmitted power versus source angle graph and also for source angle 25°-45° to get a graph for electric field intensity versus source angle.

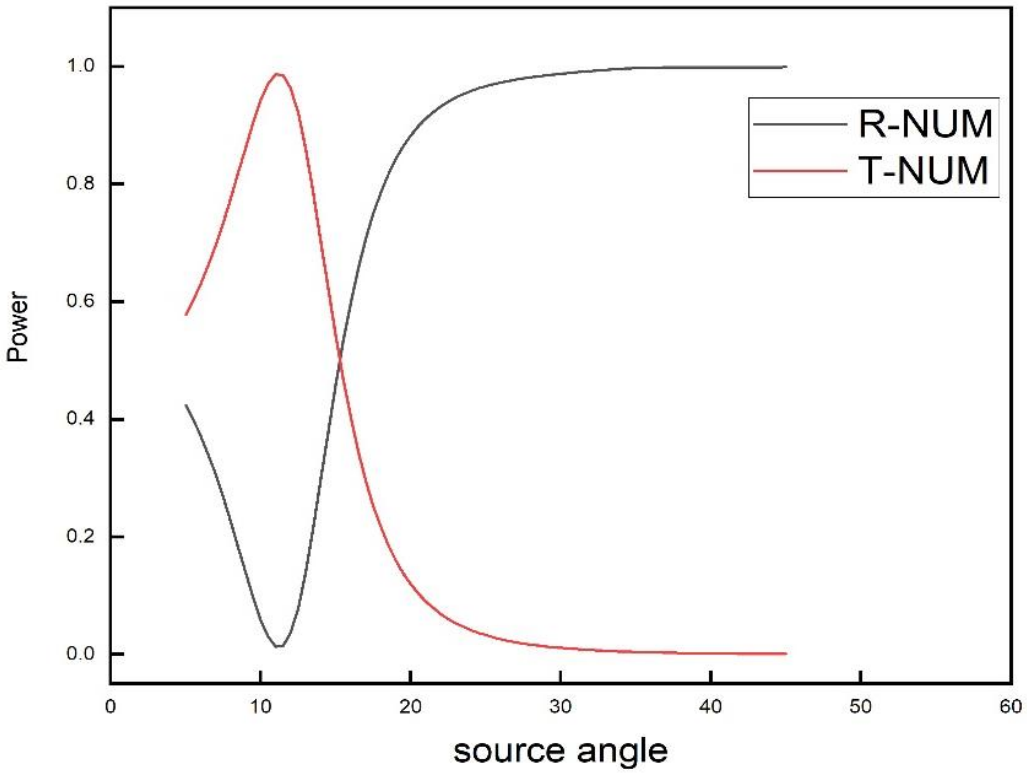

Figure 20: The plot of reflected and transmitted values as a function of source angle using Ti substrate.

From the graph (Figure 20), we can see that it doesn't match our analytical results. In the reflected power there should be a dip at source (θ_{sp}) because of evanescent field effect. On another graph (Figure 21) the electric field intensity for (θ_{sp}) is much lower which is not desired. Electric field intensity must be strongest at $\theta_{sp.}$

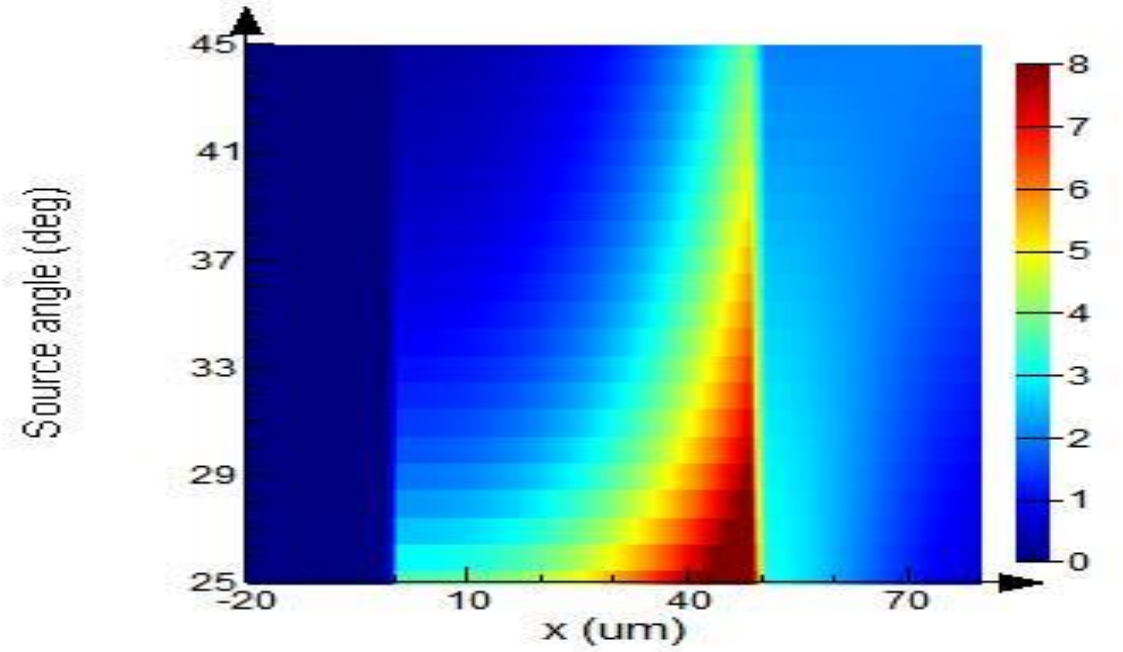

Figure 21: The electric field intensity with respect to source angle using Ti substrate.

From the plots we get the numerical values of the transmitted and reflected power values. Here we also measure the peak points for source angle 24 deg and fall points for the source angle 31 deg using all substrate (Table 1). We can see that when we excite a p polarized surface plasmon using glass substrate the reflectance power gets higher around source angle 24 deg, then it starts to decrease because of evanescent field created inside the surface plasmon. And it creates a dip in the graph around source angle 31 deg. This proves that the excitation is very high around 31 degree. And the transmitted power remains quite similar from source

	Peak Point				Fall Point			
Particle	Transmitted (Numerical)		Reflected (Numerical)		Transmitted (Numerical)		Reflected (Numerical)	
	Source angle(theta)	Power	Source angle	Power	Source angle	Power	Source angle	Power
Glass	24	0.00208	24	0.99855	31	0.00001	31	0.86165
Ti	24	0.03271	24	0.97113	31	0.00698	31	0.98825
Si	24	0.03220	24	0.96573	31	0.00697	31	0.99263

Table 1: Comparisons of using Glass, Silicon and Titanium as substrates in the p-polarized surface plasmon on graphene.

angle 24 deg to 45 deg. On the other hand, when we use silicon and Titanium instead of glass substrate, we can see there is no big change in the reflected power for the source angle 24 deg to 45 deg. And also, the transmitted power remains quite similar for the source angle 24 deg to 45 deg. As there is no dip occurs in the transmitted power and it remains similar for both transmitted and reflected power for the source angles, we can say the excitation is very weak over the surface plasmon. For that reason exciting a p polarized surface plasmon using glass substrate gives us the strongest excitation[34, 35].

3.5 Conclusion

At first, for s-polarized surface plasmon we take incident angle analytically. Then from Lumerical FDTD, we find the numerical angle. Here each incident angle is a match. In the reflected power, there is dip occurs. That is due to evanescent wave. Because, evanescent wave excites the surface plasmon, and the reflected power decreases with the increase of source angle. We also find that; the source angle of the plane wave is bigger than the TIR angle[38]. We also find very high concentration of electric field intensity at source angle. So, in source angle excitation is strongest and electric field intensity is very high. For p-polarized surface plasmon we choose 3 different substrates (Glass, Si, Ti) for this. For the glass, we find match in source angle for both numerical and analytical values and we saw dip in the reflected power around the source angle due to evanescent wave. Total internal reflection is less than the source angle. We also find, electric intensity is very high around the source angle. But for the Ti and Si, we don't find ant match between numerical and analytical values. Electric intensity is also not that high around the source angle. So, both Ti and Si substrate is not perfect for graphene P-polarization. Also, there is no dip in reflected power around the source angle. So, surface plasmon excitation is very week. Therefore, we can say using a glass substrate in p-polarized surface plasmon gives us strongest excitation and spp.

Chapter 4

Optical Absorption in Graphene Sheet

4.1 Introduction

In this Chapter we found that optical absorption in a monolayer graphene sheet is 2.3%, which is universally constant for Graphene. Then, we tried to find complete light absorption (100%) under total internal reflection (TIR) in a periodically patterned doped graphene nano-disks array[4].

4.2 Optical Absorption Coefficient in Graphene Based Monolayer

4.2.1 Introduction

We considered a single layer of carbon atoms which is known as a two-dimensional graphene material[4]. It is arranged in a shape of honeycomb lattice[4]. This 2D graphene structure exhibits a very strong light matter interaction from the near infrared to the ultraviolet region possessing a with very different wide range of frequencies and wavelengths[4, 40]. However, in graphene monolayer structure suspended in vacuum has 2.3% universal optical absorption value[4].

4.2.2 Literature Review

An atom thickness of graphene monolayer has considerably higher optical absorption of 2.3% and it is approximately 50 times more than mostly used same thickness gas[13, 40]. Moreover, It is not only behave like a frequency independent material but also shows no fundamental relationship to angle of incidence[40]. It can be used in optical fiber communication, optical resonators and different thermal imaging devices[40]. Therefore, we tried to see the optical absorption of a homogenous graphene monolayer sheet.

4.2.3 Simulation Setup

We used Lumerical FDTD Solutions to simulate absorption in graphene monolayer. In this simulation setup, we used a 2D rectangle shape of single layer graphene and Fermi energy level is 0.6eV.

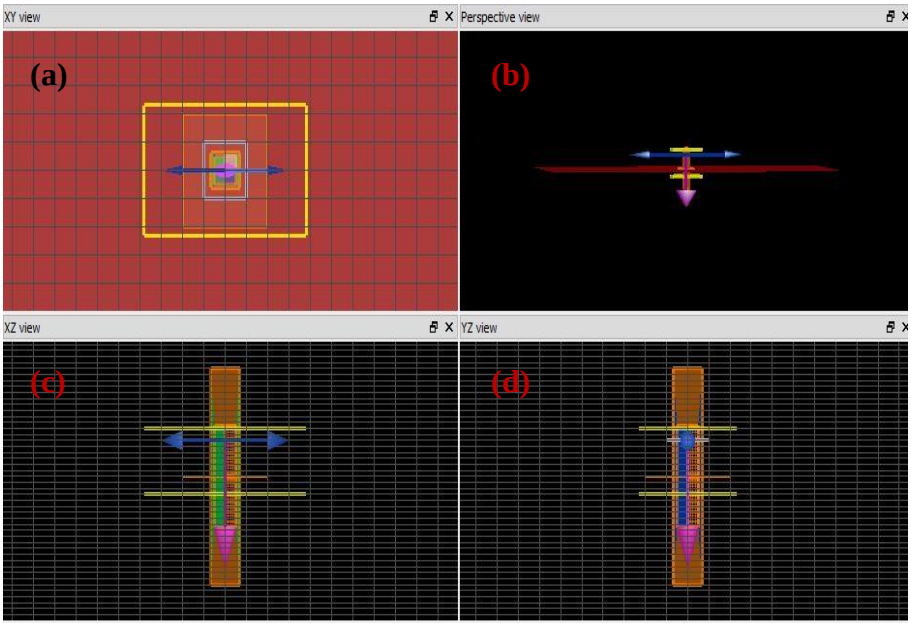

Figure 22: Simulation in FDTD solutions of optical absorption in graphene monolayer shown in (a) x-y view, (b) perspective view, (c) x-z view and (d) y-z view.

We used background index as 1, since our graphene layer is suspended in vacuum. To observe the transmission and reflection, we use two monitors. We also use a plane wave source from where the light will be emitted.

4.2.4 Results and discussion

After completing the simulation, we get the absorption coefficient vs frequency graph. From the graph (Figure 23), we see that, for lower frequency we got absorption of 10% and then it decreases to zero with the gradual increase of frequency. After that, for some times it remains constant around 0% and then again increase with the frequency. Then at around 330THz it gets to .023(2.3%) and stays constant for the rest of the frequencies.

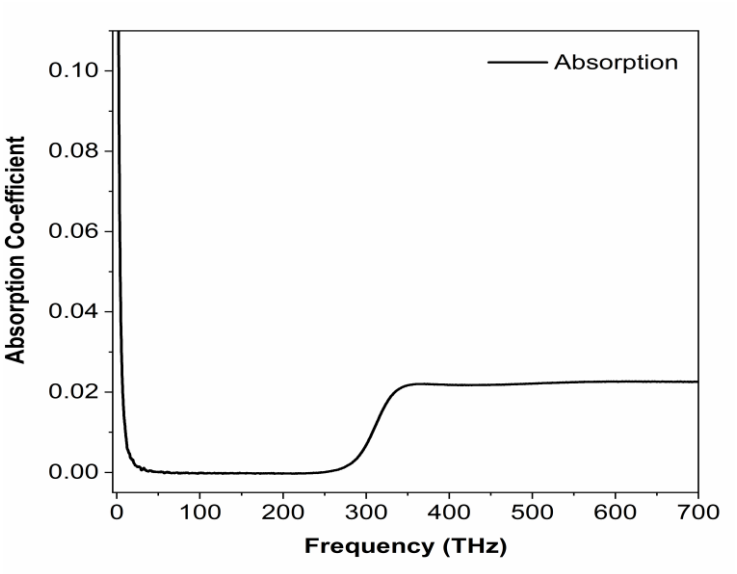

Figure 23:Absorption coefficient corresponds to frequency in homogenous graphene monolayer.

Therefore, from our simulation we can find that, the optical absorption in homogenous monolayer graphene is universally constant at 2.3%. In order to achieve 100% absorption, we considered doped graphene sheet which is described in the next section.

4.3 Total Light Absorption in Periodically Patterned Graphene Nano disk

4.3.1 Introduction

Graphene sheet can be used to design photo-detectors and photovoltaic cell due to its extraordinary characteristic of supporting strongly confined and long-lasting plasmons. Complete light absorption under total internal reflection occurs when a periodically patterned single sheet of doped graphene nano disk are placed on a dielectric coated metal[41, 42]. We attempted to calculate absorption numerically using Lumerical FDTD Solutions software.

4.3.2 Literature Review

As we have seen in the previous section that homogeneous graphene sheet holds poor absorbing behavior as absorption is only constant 2.3% [40, 43]. Because of that, we have to resort to doped graphene sheet. Doped graphene has the ability to host extremely localized, enduring plasmons where acquiring total light absorption(TLA) is very probable[44].

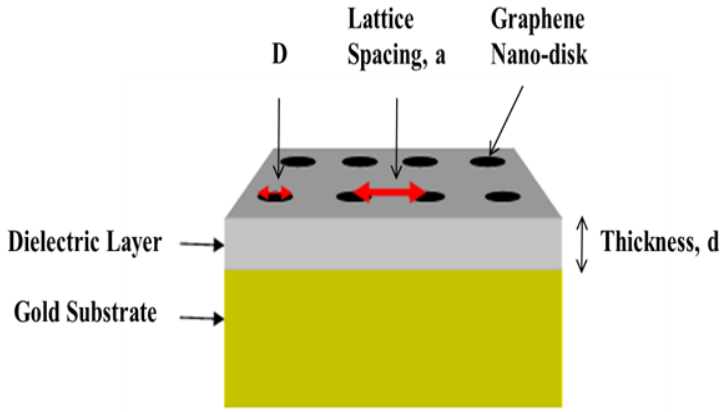

Figure 24: Scheme of periodically patterned graphene nano-disks array supported on dielectric coated gold substrate.

In the approach of achieving 100% absorption, a system has been designed where a graphene nano disk array is supported on a thick gold substrate (Figure 24). Here, we use gold substrate as a back-gate component to dope our graphene nano disk[41]. However, surface plasmons disappear at the graphene/metal interface, therefore, a intermediate dielectric coating layer has been introduced to solve the issue[13, 42]. SiO_2 layer is used as the dielectric coating in this design.

In this configuration, the thickness of SiO_2 layer is kept at least four of times smaller than the light wavelength. Diameter of a graphene nanodisk has been chosen to be 60nm and lattice spacing has been chosen to be 120nm initially[45]. The relationship between absorption,

incidence angle and polarization is very weak in this configuration, which is hinting the omnidirectional absorption[13].

4.3.3 Simulation Setup process

We constructed similar structure in Lumerical FDTD Solutions software where we considered a thick Au substrate having thickness of 11200nm and thin sio_2 layer having thickness of 800nm initially. Optical material chosen for gold is "Au- Johnson Christy"

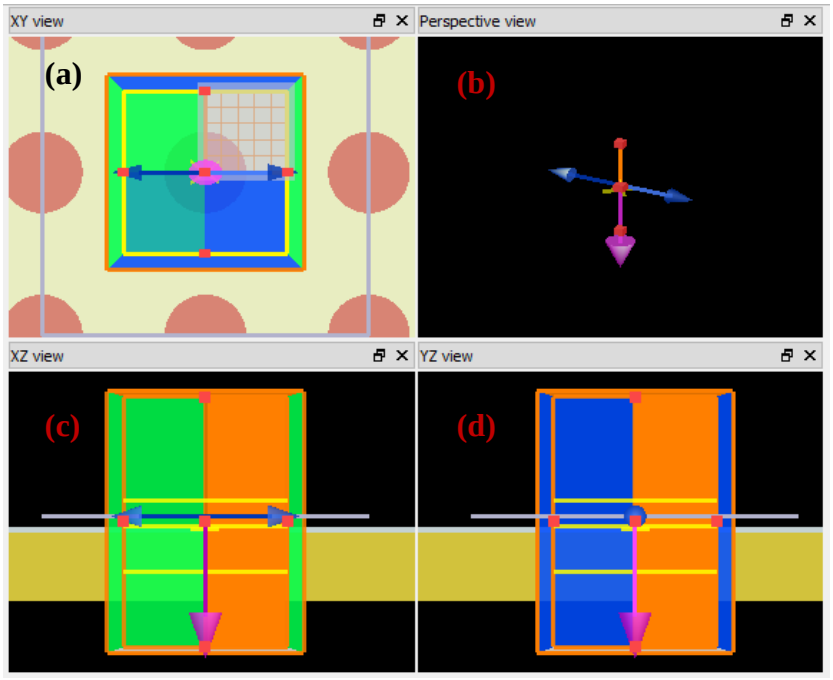

Figure 25: Simulation in FDTD solutions of optical absorption in periodically patterned graphene nanodisks shown in (a) x-y view, (b) perspective view, (c) x-z view and (d) y-z view.

whose refractive index is 0.92 in the near-infrared region[15] and the optical material chosen for sio_2 is "Si- Palik" whose refractive index is around 2.7 in the near-infrared region. The optical material chosen for graphene nanodisk is "Graphene Broad Band" whose chemical potential (Fermi energy level) is 0.4ev, scattering rate is 0.00012ev and refractive index is 3.1 in near-infrared region.

The radius of each nanodisk was chosen to be 30nm and the lattice spacing was 120nm. A plane wave source has been considered where the wave is propagating along –ve z direction. The incidence angle was chosen to zero degree as incidence angle dependency on absorbance is very weak. FDTD simulation region was 120nm along x direction, 120 nm along y direction and 40,000nm along z direction where number of mesh cells used along x and y axes is 10 units each and 2000 mesh cells along z axis. We set the periodic boundary condition along with the x and y axis as the structure is periodic along xy plane and PML(Perfectly Matched Layer) boundary condition is being used along z axis as the EM wave is propagating along z direction[46]. Two DFT monitors were used to determine the reflected power and transmission power after EM wave incidents on air/graphene surface.

4.3.4 Results and discussion

Initially, thickness of the dielectric coating layer was set to 800nm and tried to find reflection, transmission and absorption for this design[47].

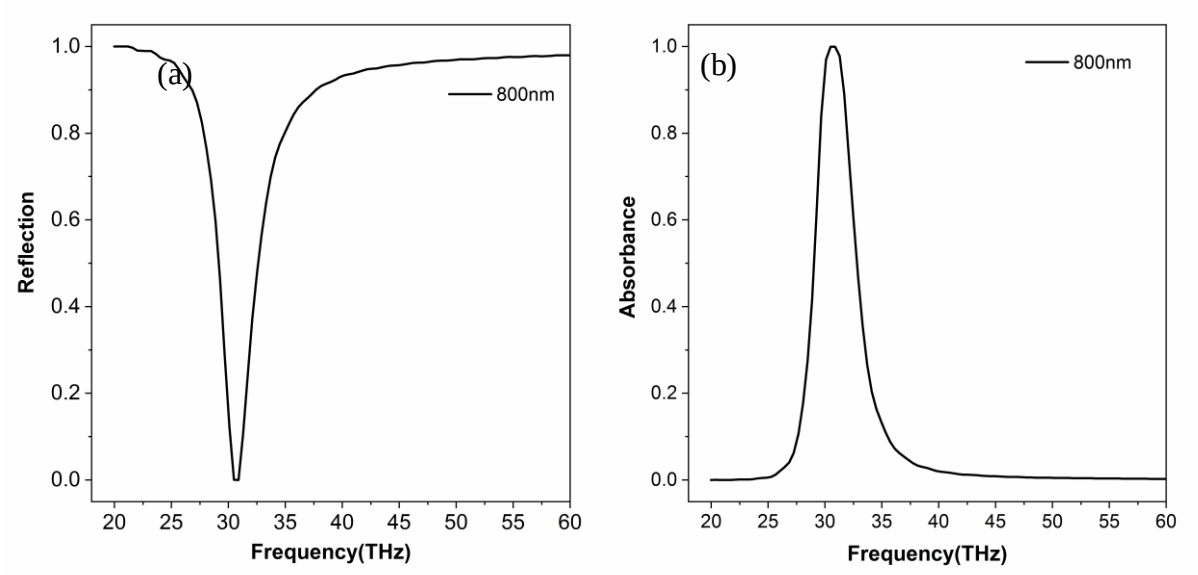

Figure 26: (a) Normal incidence reflection and (b) Normal incidence absorption, by graphene disk arrays on dielectric coated gold surface[13].

In the reflection curve [Figure 26(a)], we observed that transmission channel was suppressed (Transmission=0) as Total Internal Reflection (TIR) occurred. A prominent absorption dip was seen around frequency of 31 THz, so near-Infrared (IR) the light is absorbed by the graphene surface plasmons[38]. In the absorption curve [Figure 26(b)], we observed that Total Light Absorption (TLA) is attained at 30.8 THz frequency when the thickness of dielectric layer is 800nm.

Then, we varied the thickness of dielectric layer to observe the relationship between the absorption in graphene nanodisks and the thickness of SiO_2.

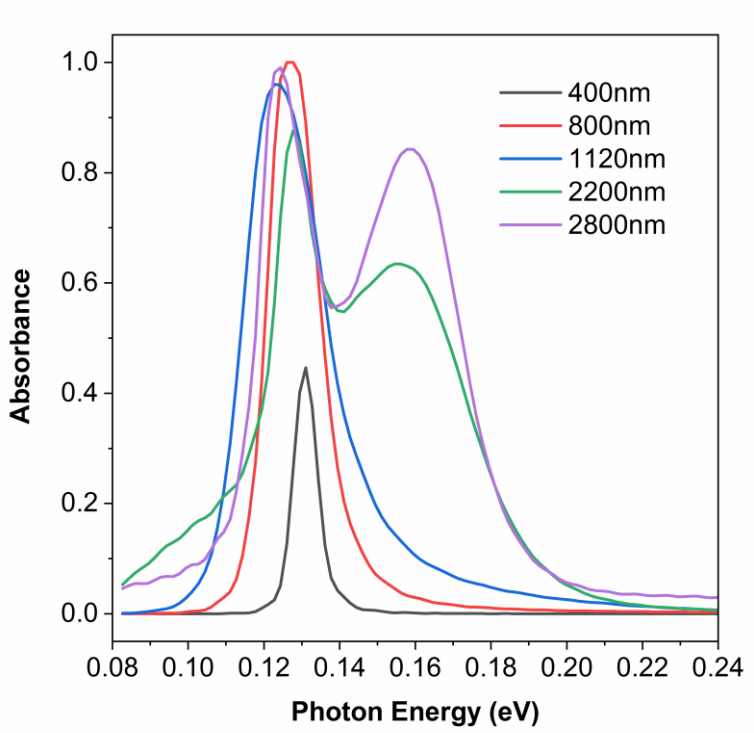

Figure 27: Normal incidence absorption by graphene nano-disks arrays on dielectric coated gold surface for various values of the dielectric film thickness[13, 41].

From Figure 35 and Table-2, it is very prominent that absorbance is maximum when the dielectric layer thickness is 800nm, in other cases the absorbance varies from 0.446 to 0.989. Again, the SPR peaks are located within very small range of energy (0.124ev ~ 0.131ev). As

we increase the thickness of dielectric layer, when the thickness is above 2000nm multiple modes are observed in the absorption curve. For example, when the thickness is 2200nm, two different modes are observed, the center position of the mode 1 is at 0.128 eV where we have higher absorbance (0.876) and for mode 2, the absorbance is 0.642 and the center position is at 0.155eV [48].

Thickness of SiO_2	**Peak Index**	**SPR Peak (ev)**	**Absorbance**	**FWHM (ev)**
400 nm	-	0.131	0.446	0.009
800 nm	-	0.128	0.999	0.016
1120 nm	-	0.124	0.959	0.020
2200 nm	1	0.128	0.876	0.018
	2	0.155	0.642	0.040
2800 nm	1	0.124	0.989	0.022
	2	0.158	0.845	0.040

Table 2: Comparison between SPR Peak(Center), absorbance and FWHM in the absorption curves due to various values of the dielectric film thickness.

Then we compared our numerically calculated results with the literature [6] where they followed analytical method while doing calculations. From Table-3, we can see that, the SPR

Thickness of SiO_2	**SPR Peak (eV)**		**Absorbance**		**FWHM (eV)**	
	Numerical (FDTD Solutions)	**Analytical (Literature)**	**Numerical (FDTD Solutions)**	**Analytical (Literature)**	**Numerical (FDTD Solutions)**	**Analytical (Literature)**
400nm	0.131	0.135	0.446	0.38	0.009	0.002
800nm	0.128	0.134	0.999	0.90	0.016	0.0024
1120nm	0.124	0.135	0.959	0.999	0.020	0.004
2200nm (mode 1)	0.128	0.136	0.876	0.95	0.018	0.004

2800nm (mode 1)	0.124	0.135	0.989	0.26	0.022	0.002

Table 3: Comparison of the results between FDTD Solutions and the literature[6].

peak positions in our results are almost same as in the literature, absorbance is also similar for both cases, but the FWHM found in our results is bit wider than the analytically calculated curves in the literature.

After that, in order to observe coupling effect in the graphene nano-disks, we were gradually decreasing the value of lattice spacing which was 120nm initially and while varying lattice spacing, we kept the dielectric layer thickness at 800nm.

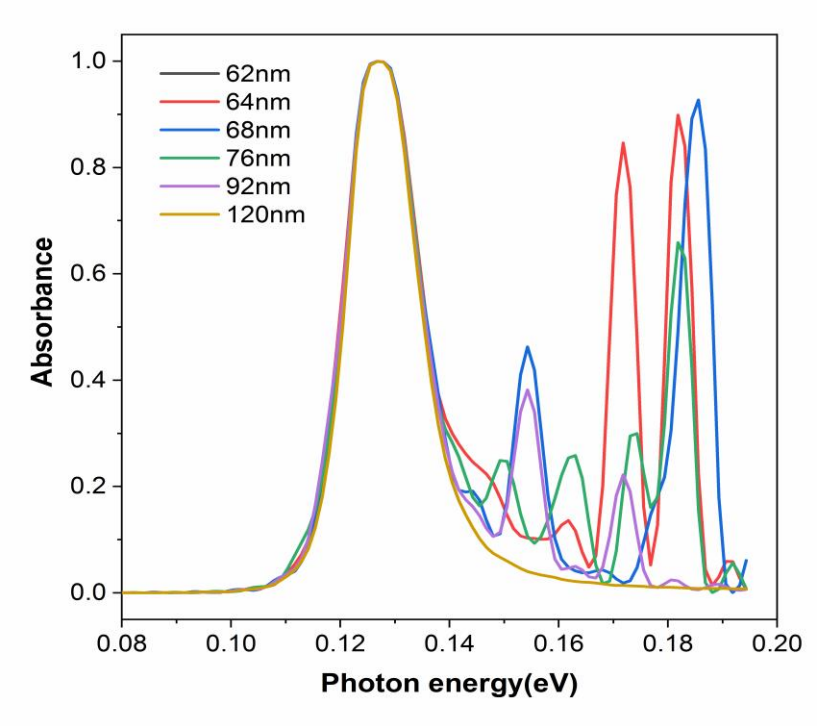

Figure 28: Normal-incidence absorption by graphene nano-disks arrays for various values of lattice spacing of graphene nano-disks.

From Figure 28, when the lattice spacing gets decreased, we were observing multiple modes instead of a single mode. In Table 4, we compared each absorption curve with one-another on basis of SPR Peak positions and absorption intensity of the multiple modes. When the lattice

spacing is at minimum, we observed at most 5 different modes at 0.128eV, 0.153eV, 0.162eV, 0.172eV and 0.183eV center photon energy.

	Peak index	Lattice spacing, a=120nm	Lattice spacing, a= 92nm	Lattice spacing, a=76nm	Lattice spacing, a= 68nm	Lattice spacing, a= 64nm	Lattice spacing, a= 62nm
SPR Peak/ Center (eV)	1	0.128	0.128	0.128	0.128	0.128	0.128
	2	-	0.153	0.153	0.153	-	-
	3	-	-	0.162	-	0.162	0.162
	4	-	0.172	0.172	-	0.172	0.172
	5	-	-	0.183	0.183	0.183	0.183
Absorbance	1	0.999	0.999	0.999	0.999	0.999	0.999
	2	-	0.38	0.25	0.47	-	-
	3	-	-	0.25	-	0.14	0.14
	4	-	0.23	0.31	-	0.83	0.83
	5	-	-	0.66	0.93	0.88	0.88

Table 4: Comparison between absorption curves due to various value of lattice spacing of graphene nano-disks.

4.4 Conclusion

Therefore, we have observed 100% light absorption is achievable by periodically patterned doped graphene nano-disks, whereas we previously observed that only 2.3% absorption occurs due to a single sheet of homogenous graphene, which is a big step ahead in order to manufacture graphene-based IR photodetectors, narrow-band IR source and photovoltaic cell.

Chapter 5

Electro-optical modulator (EOM) device based on a graphene coated waveguide material.

5.1 Introduction

In this chapter we demonstrate an electro-optical modulator device based on graphene coated waveguide[49]. As the electro-optical (EO) modulator is very essential element for the signal processing and optical communications now a day. Therefore, we will demonstrate a 2D model for optical simulation as well as a 3D model for electrical simulation for the modulation of the EOM device[23]. Here we try to observe the optical absorption and energy propagation through an electro-optical modulator in terms of intra band and inter band transition when we apply a bias voltage on the junction. Then we develop our understanding how the change of graphene's fermi level effect on the device when we apply Gate voltage on the graphene layer.

5.2 Electro-optical modulator

An electro-optical modulator (EOM) usually modulates a ray of light in an optical device[50]. From an EOM device a signal-controlled element exhibits electro-optical effects [23, 50, 51]. Moreover, this kind of electro-optical modulation is done by the phase or frequency or amplitude or polarization of the photon beam[50]. Modulation bandwidths of the device extends into the gigahertz range[50]. Thus it is possible that with the help of laser-controlled modulators[50, 52]. Furthermore, electro-optical modulator devices are like semiconductor devices[50]. They have very fast optical response, low loss, compact in their size, wide bandwidth and many power saving properties[53]. Those properties are more popular for on chip optical interconnects[51, 54]. Silicon, InP, Ge and other nonlinear polymers are used to

construct the electro-optical modulators[53]. Despite having all those benefits many electro-optical modulators suffer from large transmission losses, their bandwidth is very small, and also they have low thermal ability[53, 55]. Therefore, a graphene based electro-optical modulator which has low operation voltage, compressed in size, , ultrafast modulation speed can help us for on-chip optical communications and low power consumption application of EO modulation[23, 51, 55]. In this experiment we will demonstrate an electro-optical device for a graphene coated waveguide.

5.3 Literature review

A single sheet of graphene has exceptional and great electrical and optical properties rather than other material[56]. A graphene monolayer always shows a constant absorption rate of 2.3% from visible range to the infrared range of wavelengths [57, 58]. Due to the wide bandwidth, low electric density, fast modulating and low power consumption characteristics of graphene, we design an electro-optical modulator structure based on graphene[23, 51, 58]. For that reason, we use a CMOS structure[54]. We demonstrate the high modulation rate of the guided light by changing the fermi energy level or chemical potential of graphene [11, 23, 51].

The optical absorption and transmission are inversely proportional to each other. We achieve our desired absorption or transmission rate of the modulator (Figure 29) by electrically[23]. There we change the chemical potential or fermi energy level of the graphene layers by applying bias voltages [3, 23, 51]. When there is a high applied voltage, the fermi energy level stays very low from valance band edge. Therefore, the valance band and conduction band stay empty and there will be no optical absorption happened[23, 51]. Then, when the applied voltage is close to zero, the fermi energy level stays in the equilibrium position[59]. In this condition electron in the valance band get excited by the photon energy and jumps to

the conduction band where the EHP (electron hole pair) generation occurs and the light gets absorbed. So, the transmission of photon is lower and the absorption rate is very high[51]. Then again, when the applied voltage is very low, the Fermi Energy level stays very high from conduction band. The conduction band and the valance band stay full. So, there will no EHP generation or absorption of photon in the device[23]. Therefore, by changing graphene's fermi energy level we can get our desired modulation from the electro-optical modulator[51,

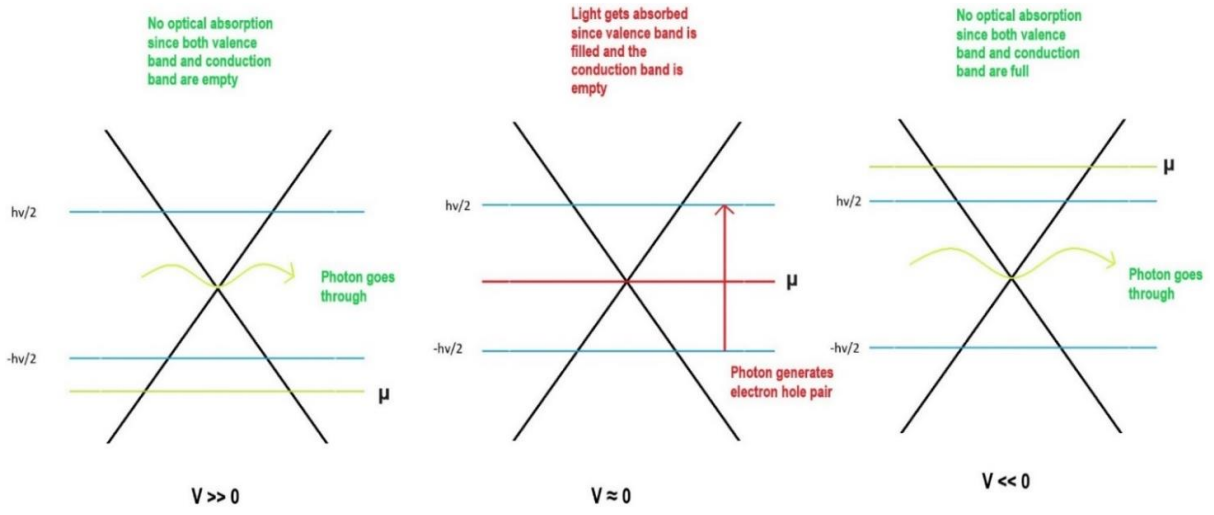

Figure 29: Modulation process in graphene's optical absorption by applied bias voltage.

60, 61]. As we know from the electrical properties that graphene shows zero density of states when it reaches at the fermi dirac position[9]. Therefore, the electric conductivity will stay very low which is not desired[9]. To overcome this problem, we change the fermi level by doping waveguide material with boron to reduce the graphene sheet resistance and also to create a new material that would be better at conducting electricity[9, 51, 60].

The 2D Density of states (DOS) of graphene can be calculated by,

$$g(E) = \frac{2|E|}{\pi \mathrm{H}^2 v_F^2}$$

Here, the fermi velocity in graphene, v_f = 106 m/sec and E is the electron energy[23].

For any 3D semiconductor the DOS is calculated by,

$$g(E) = \frac{\sqrt{2}}{\pi^2}\left(\frac{m^*}{\mathrm{H}^2}\right)^{3/2}\sqrt{E - E_c}$$

Here,

m* = Effective mass of the electron and hole and

Ec = The minimum conduction band edge energy[23].

We also calculate the 2D electron density (/cm2) for the zero-bandgap graphene by using,

$$n_{2D} = \int_0^\infty g(E)f(E)dE = N_{c,2d}\int_0^\infty \frac{E}{1 + \exp\big((E - E_F)/(kT)\big)}dE$$

$$n_{2D} = N'_{c,2d}\int_0^\infty \frac{\varepsilon}{1 + \exp(\varepsilon - \eta)}d\varepsilon = N'_{c,2d}F_1(\eta)$$

Here, $\varepsilon = E/(kT)$,

2D effective DOS $N'_{c,2d} = \frac{2(kT)^2}{\pi \mathrm{H}^2 v_F^2}$,

Fermi level = EF,

Boltzmann constant = k,

Temperature = T,

F1(η) = 1st order fermi dirac integral where, η=EF⁄kt [23].

Then we calculate the 3D electron density (/cm3) of a semiconductor by,

$$n_{3D} = N'_{c,3d} \int_0^{\infty} \frac{\sqrt{\varepsilon}}{1 + \exp(\varepsilon - \eta)} d\varepsilon = N'_{c,3d} F_{1/2}(\eta)$$

Where,

F1⁄2 (η) =1/2 order fermi-dirac integral where, η=(EF-Ec)/kt,

E_F = Fermi level,

Ec= Energy at the minimum conduction band edge,

3D effective DOS $N'_{c,3d} = \frac{1}{\sqrt{2}} \left(\frac{m^* kT}{\pi h^2} \right)^{3/2}$,

m* =The electron effective mass [23].

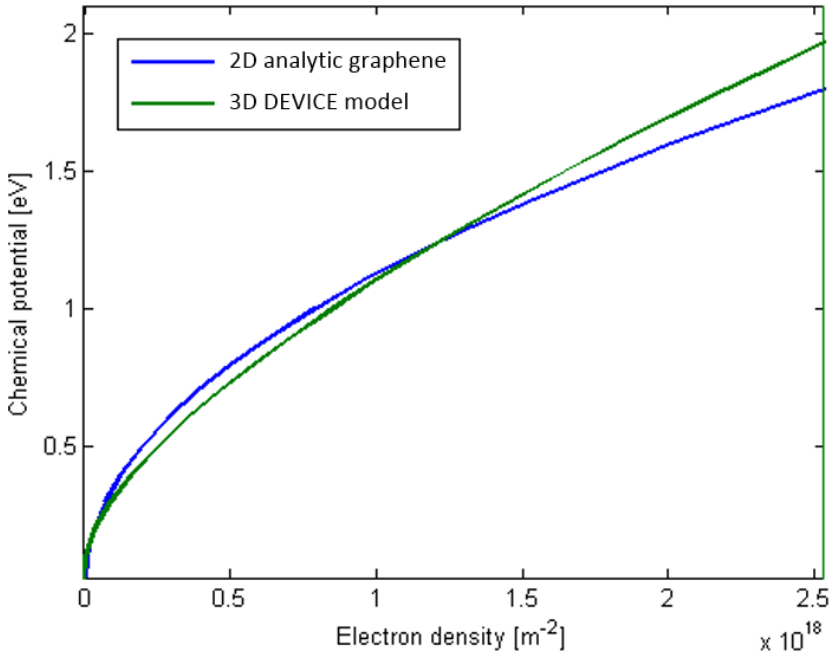

Figure 30: Electron density comparison of 2D(Analytical) and 3D(Experimental) graphene sheet [23].

The Figure-30 shows that after calculating the electron density where we used

m*=1.768,

Ec=0.1eV [23]

And also found out that a 1 nm thick 3D graphene sheet shows better electron density (/m2) than analytical 2D graphene electron density [23, 51].

5.4 Simulation setup process

In our structure (Figure 31), we use two coats of graphene layers [23]. One coat is used on the top of the Si and another one is used on the side wall of the Si waveguide core[23]. The core with the graphene layer is separated with 7nm Al_2O_3 [23]. We use SiO_2 at the bottom as a substrate of the structure[23]. Here we are using 15 meV scattering rate and 300K temperature[23]. Furthermore, we doped both of the silicon layer and the waveguide core with an boron at a concentration of 10^{18} /cm^3 [23]. Thus, it will help to reduce the sheet resistance in the Electrical setup[23, 51].

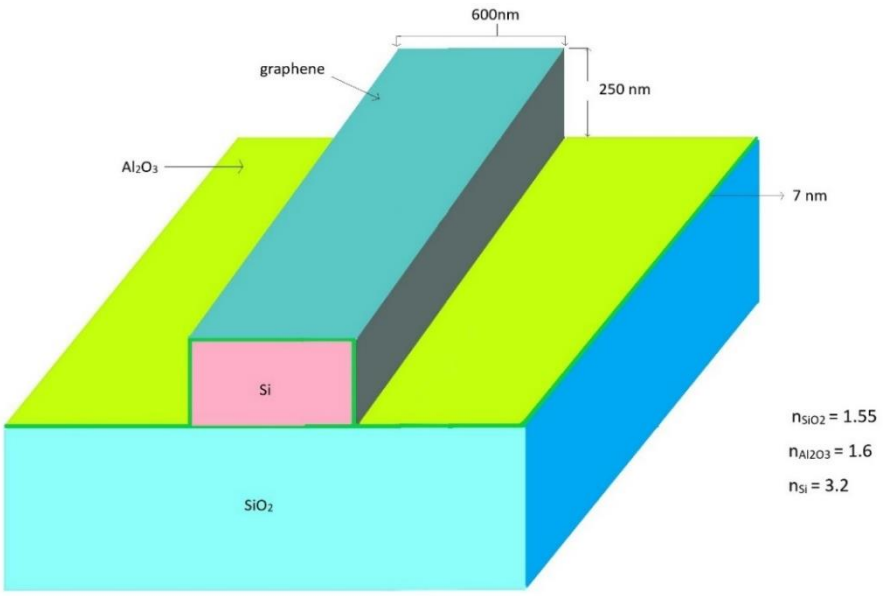

Figure 31: Electro-Optical modulator structure[23].

We use lumerical mode Solution software for Optical simulation part and Lumerical DEVICE Solution for Electrical simulation part. We combined the optical and electrical data and design a Electro Optical modulator.

5.4.1 Optical simulation process

We use Lumerical MODE Solution software setup our experimental setup (Figure 32). First of all, we build a 2d finite difference eigenmode (FDE) structure and then we simulate the structure at the minimum absorption states and also at the maximum absorption states for better modulation results [23]. We model the minimum and maximum states in two different sets of chemical potentials which are used in the structure are shown in the table-5 [23].

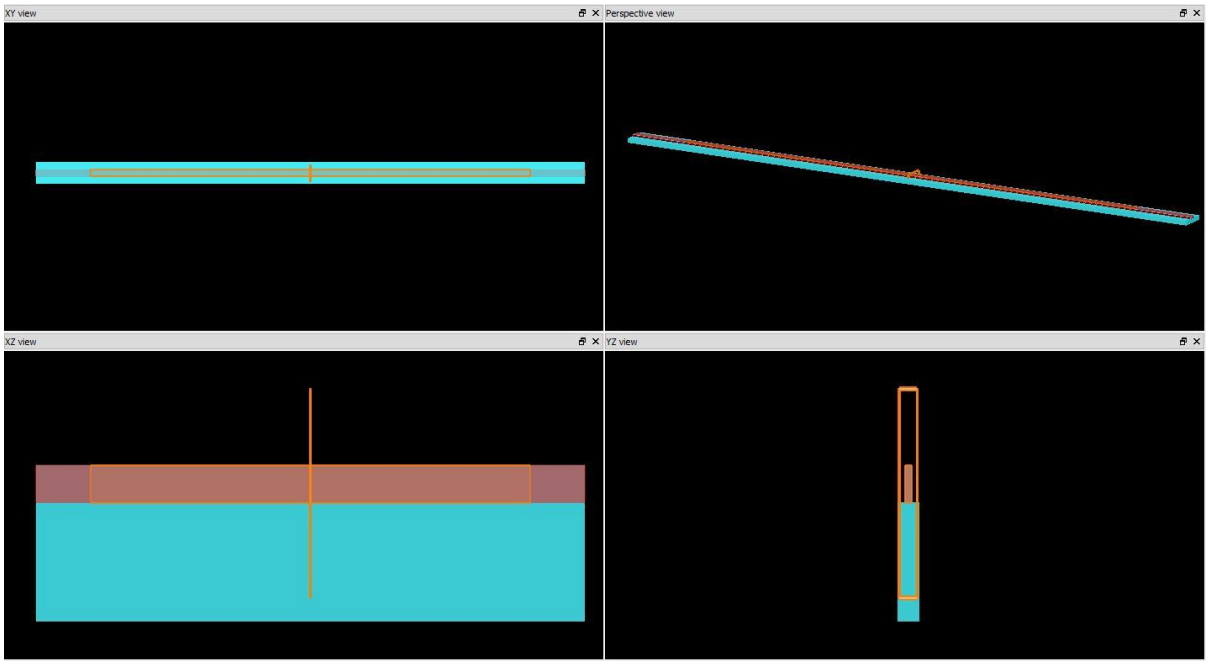

Figure 32: Optical simulation setup in Lumerical MODE Solution software.

The mode of the structure is configured with the effective index of 1.78 at 1.53 wavelength for our desired result [23]. Moreover, we set various chemical potentials to see the change in fermi energy level for top sheet and bottom sheet of the graphene at minimum and maximum absorption states[23]. This will lead us to get the cross sectional electric field of the mode [23].

Chemical potential used for	At minimum absorption rate	At maximum absorption rate
Top sheet of graphene	0.516 eV	0.0930 eV
Side sheet of graphene	0.560 eV	0.0103eV

Table 5: Chemical potential used for the top sheet and side sheet of graphene at minimum and maximum absorption rate[23].

Then we simulate our 3D bi-directional eigenmode expansion (EME) structure for calculating the 3D electric field distribution [23]. Therefore, we found the electric field propagation along the x axis for the minimum absorption states and then for the maximum absorption states showed in table-5 earlier [23]. Finally, we import electron-hole density material attributes from our electrical simulation for the improvement of loss generated from our structure [23]. There we use a volumetric material model in the electrical simulation setup and then we calculate the electrical properties of graphene surface for our structure [23]. After that we get the losses for each biasing voltage applied into the modulator[23].

5.4.2 Electrical simulation process

We model the graphene here using Lumerical CHARGE software to observe the electrical properties at different states for the change of fermi energy level [23]. In the lumerical CHARGE solver we can easily calculate the electrical properties of graphene-based structures by using a 3D density-of-states model as well as an effective-mass for the material [23]. However, we use different types of parameters and chemical potentials for getting the perfect transmission and absorption rate results for the model [23].

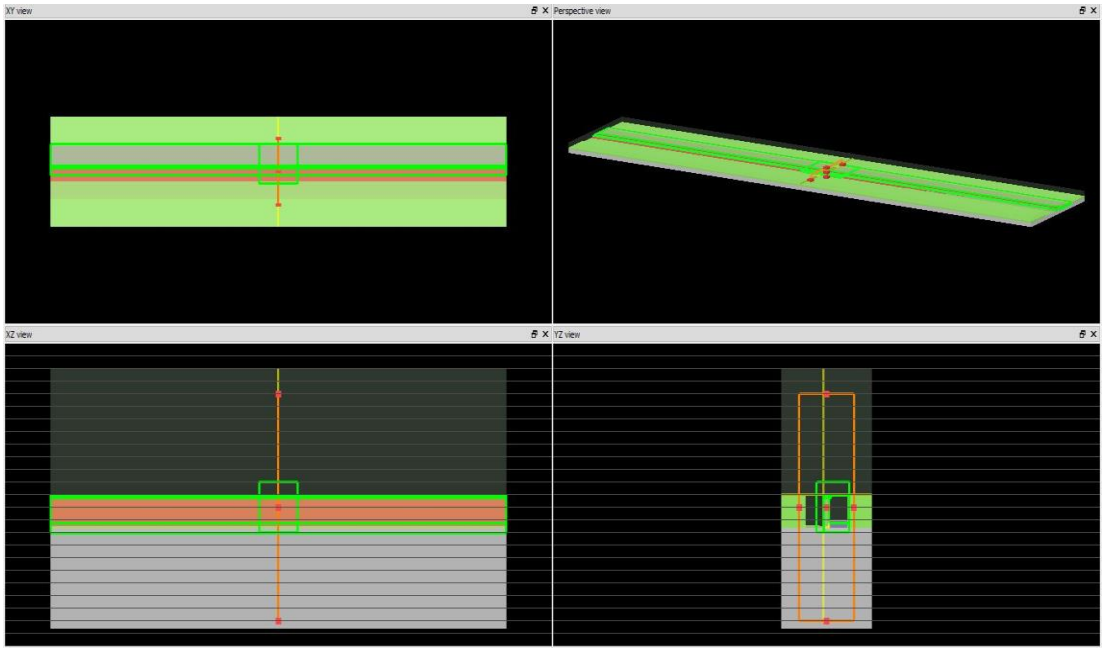

Figure 33: Electrical simulation setup in Lumerical Device Solution software.

Here we change the Fermi Energy level by applying bias voltage for E_f<= .5ev and E_f>.5ev of graphene. In both cases we doped the silicon waveguide with Boron acceptor concentration 10^{18} / cm^3. For both graphene structure we use same conduction band minimum, but different Fermi level, m* (electron or hole effective mass) and thickness[23].

Model	**Graphene_1 ($E_F \leq$ 0.05 ev)**	**Graphene_2 (E_F > 0.05 ev)**
Range of E_F (ev)	≤ 0.05	0.05
M*	1.768	0.4614
E_c (ev)	0.1	0.1
Thickness of graphene sheet (nm)	0.1	0.75

Table 6: Parameters used for 3D equivalent electrical models of graphene in Electrical setup.

Moreover, for both structures we use two band structure monitors to record the chemical potentials or the fermi levels of the graphene sheets (Table 6) [62]. We use Au(Gold) as the

base and gate to supply voltage in the modulator. We observe the change in the chemical potentials of the graphene sheets on top of the waveguide and also on left wall of the waveguide due to different applied gate voltages [23]. Then we merged those datas get from the Electrical simulations with the optical simulation [23].

5.5 Results and discussion

5.5.1 Optical simulation result

First of all, we run the 2D FDE simulation structure and then we get the cross sectional view of the electrical field propagation of the 2D structure[23]. Moreover, we also found that there is some transmission losses generated in the medium and recorded as minimum 0.0113 db/μm and maximum 0.117 db/μm [23]. Furthermore, the modulator's cross sectional field

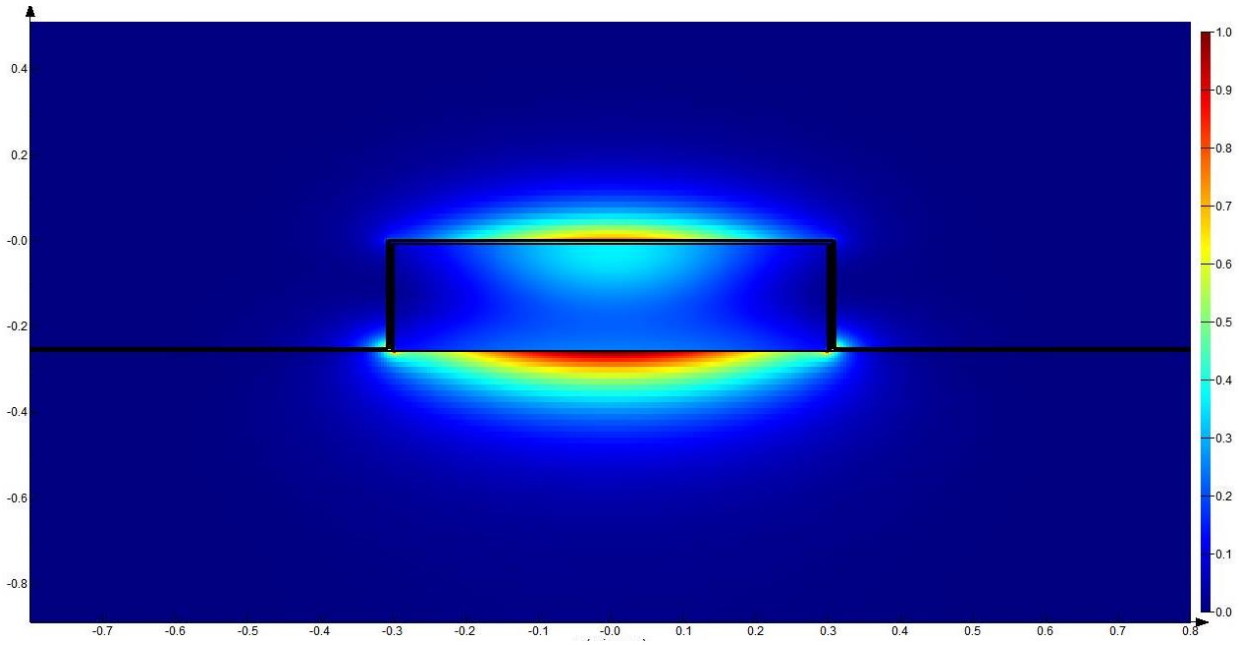

Figure 34: The cross sectional view of electric field for the minimum and maximum absorption states.

is quite same for different absorption states and it would help us to operate the modulators waveguide efficiently (Figure 34) [23].

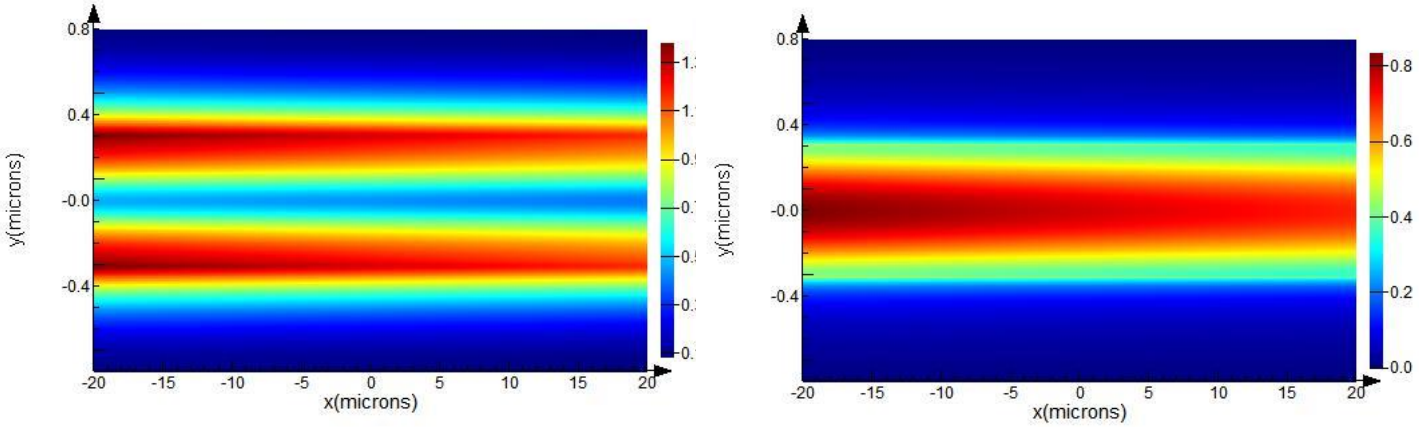

Figure 35: Electric field propagation for minimum absorption rate shown at left and for maximum absorption rate shown at right.

After that, we simulate the 3d EME structure and get the we get the electric field distribution along x axis for different absorption states showed in Figure-35 [23]. However, we can see there is a change in electric field distribution in 3D model along the propagation direction and also some transmission losses with respect to 2D FDE model[23].

Furthermore, we have to model a perfect optical response of the modulator with proper bias dependent[23]. To do so, we import the calculated the density of electron and hole distribution from electrical simulation result and put those into the optical simulation setup for observing the changes[23]. Moreover, we also implement the chemical potential values of the electrical simulation result in this optical simulation setup[23]. Then we run the 2D simulation and we get the transmission losses for different applied bias voltages[23]. Here, we try to achieve modulation by changing the fermi energy or chemical potential of the graphene layers for different applied voltages and observe its optical absorption rate[51, 60]. However, the optical response of silicon waveguide also gets modulated by the optical

absorption rate of the graphene. We use the results from our Electrical simulation and combined those with the Optical simulation and also get a plot for the Electro-Optical response[23].

From the Figure-36 we can observe the transmission loss and absorption of the device at different applied voltages [23]. Moreover, we can see the transmission and absorption change can be controlled by using different gate voltages. Here, in the left region where V<-1V the fermi energy level is staying lower than half of the photon energy and so there will be no electron available for the intraband optical transition [51, 54]. Therefore, the transmission of

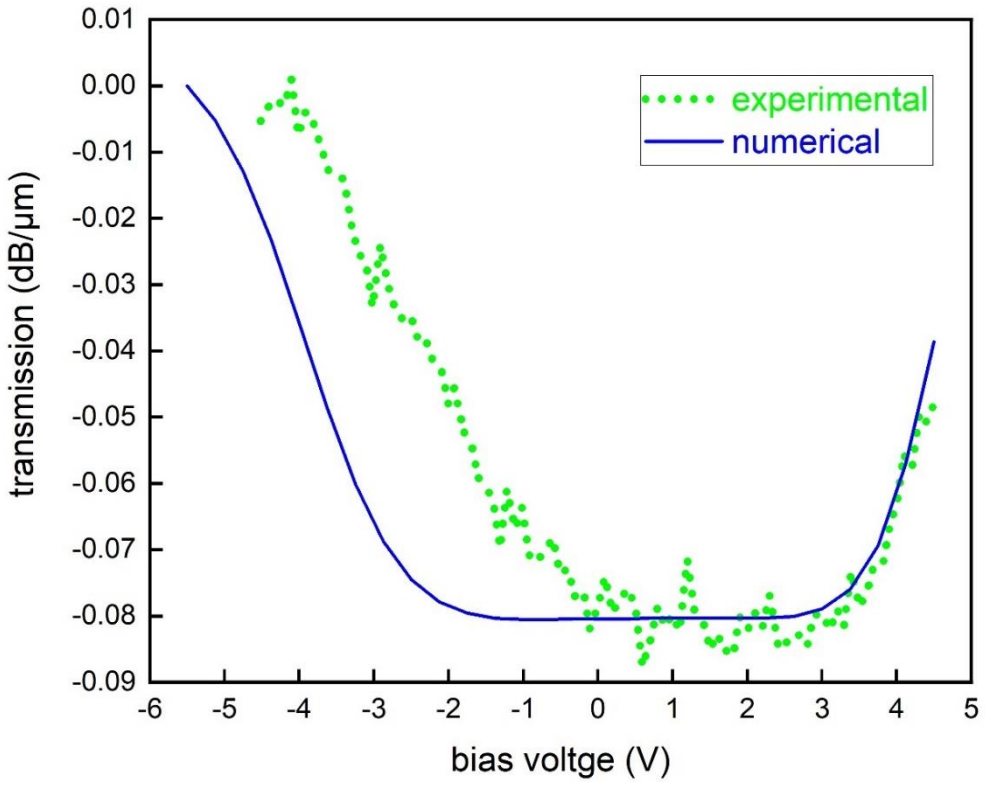

Figure 36: Experimental results and approximation results of the modulator shows when V<1V energy transmission is very high, when -1<V<3.8 energy transmission is low and when V>3.8V energy transmission is gets very high in the modulator.

photon is higher in this region[51, 54]. Then, in the middle region -1<V<3.8 where the fermi energy level is close to the fermi dirac position and the electron in conduction band get energized by photon energy[51, 54]. So here intraband optical transition is occured from occupied electron region to the unoccupied region [51, 54]. Therefore, the transmission of photon is low in this region because of absorption. And in the right region where V>3.8V, the fermi level stays above the half of the photon energy and all the electron states are occupied [51, 54]. Therefore, the intraband transition of electron an hole is not allowed in this region and photon transmission gets high[51, 54].

From the figure-36 we can see that the experimental results is quite similar to our approximate data [23]. Therefore, from the optical results we can say that we can control the photon energy absorption and transmission by changing the fermi level of graphene layer[51].

5.5.2 Electrical simulation setup results

When we apply different bias voltage in the modulator where we doped Si wave guide with Boron, the Chemical potential of graphene layers of the modulator also changes with voltages[23, 51]. When Graphene and Si are brought in contact, their chemical potentials, or Fermi levels should line up together where the density of electron diffuse from higher energy level to lower energy level until the equilibrium[60, 63]. From our Electrical simulation we can observe the changes in Chemical potential of Graphene sheet at different gate voltages which we set for minimum and maximum absorption rate previously. [51, 60]

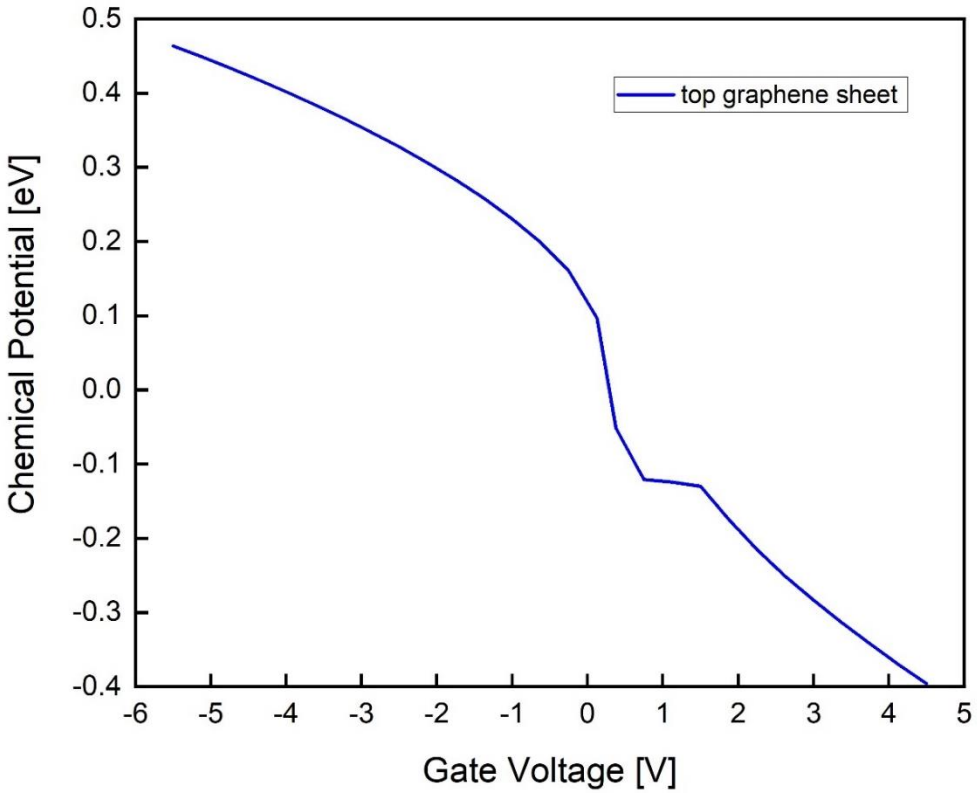

Figure 37: Chemical potential of graphene at different bias voltages for tuning fermi energy level.

From the Figure-37, we can see that the fermi energy or chemical potential of the graphene sheet is very high at the beginning and decrease linearly because of the density of electrons [51]. When we change the Fermi level for different bias voltage the chemical potential also changes. From our optical results we see the absorption of photon energy is very high near zero bias voltage [23]. In this figure-37 we can also see that near zero bias voltage fermi level or the chemical potential reached the fermi dirac point where there is a tilt in the graph because of the high absorption rate in this region [23, 61]. Then after some time the chemical potential line again decrease linearly with the bias voltage.

5.6 Designing the electro-optical modulator using different waveguide material

5.6.1 Introduction

In our previous section we develop an electro optical modulator using graphene coated Si waveguide material. In this section we will try to demonstrate the same EOM model but using different waveguide core Ge and observe the electrical and optical response of the modulator.

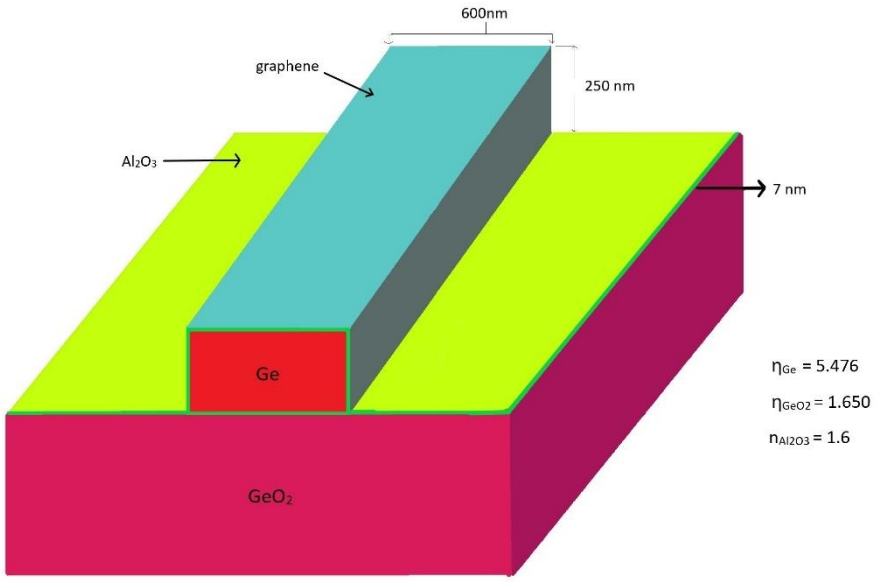

Figure 38: Electro-optical modulator structure using Ge waveguide core.

5.6.2 Electrical and Optical simulation process

In this experiment we have used the same simulation structure and parameters like before and follow the steps accordingly. Firstly, for the optical simulation process in lumerical MODE we set the same parameters and chemical potentials for minimum and maximum absorption rates showed in table-5. Secondly, for the electrical simulation process in the Lumerical

CHARGE we set the same parameters and structures of graphene showed in table-6. Then we simulate both optical and electrical structures accordingly and merged the results.

5.6.3 Optical simulation result

Firstly, from the optical simulation setup using Ge waveguide core we get the electro optical results of the transmission and absorption of photon as described in figure-29. There we learned that the transmission and absorption are inversely proportional to each other. Moreover, from the simulation graph (Figure 39) we can see that for different applied voltage the modulator is showing different transmission and absorption rates.

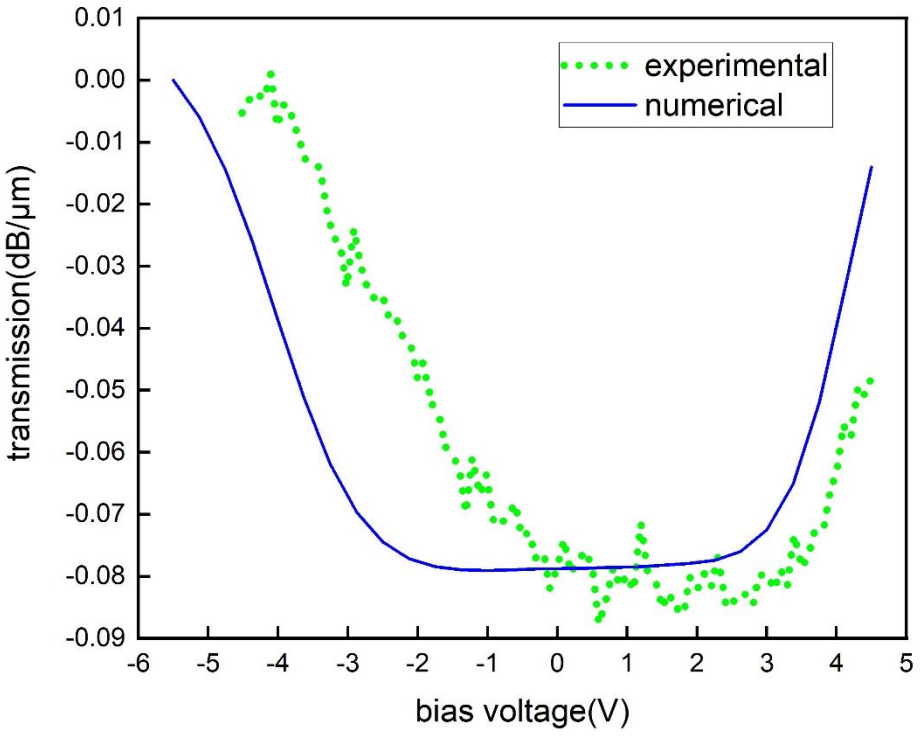

Figure 39: Optical simulation result where the transmission is showed for different bias voltages.

We can see from our experimental result which is similar to our approximated values that for V<0V transmission of photon is very high and for that the absorption rate is very low. Then for applied voltage 0V<V<3.5V transmission of photon is very low, thus the absorption rate

is very high in this region. And for the applied voltage V>3.5V the transmission of photon seems very high again and so the absorption rate in this region is very low. Therefore from our optical simulation results we can say that we can control the absorption rate and transmission rate of the modulator by applying the voltage.

5.6.4 Electrical simulation result

To control the absorption and transmission rate of the modulator we need to change the fermi energy level or chemical potential of graphene by applied gate voltage. From our electrical simulation setup, we get a plot (Figure 40) where we can see that for different applied voltage

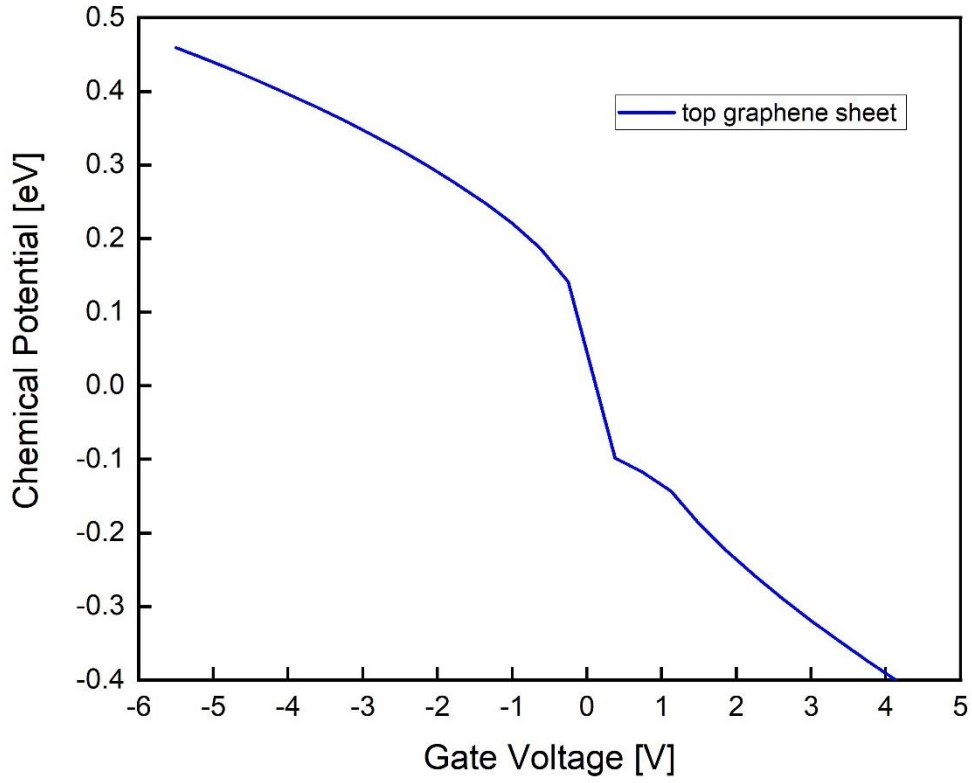

Figure 40: Change in the chemical potential of graphene at different gate voltage.

the chemical potential or fermi energy level of graphene is changing. From the figure-40 we can see that the chemical potential is very high for the applied voltage V<0V. Then when the voltage gradually increase and reaches close to 0V, it reaches the fermi dirac point. Then

again for the applied voltage V>0V the chemical potential gradually decrease and reaches the lowest point.

5.7 Conclusion

To sum up, we have developed two electro-optical modulator structure based on graphene coated Si and Ge waveguide. Both structures shows a strong photon absorption at lower biased voltage [51]. Furthermore, we demonstrated that fermi energy level of graphene can be changed by applying voltage in the modulator and it would help to control the absorption and transmission of the modulator. Moreover, its optical absorption is independent of wavelength because of the constant dirac fermions[51]. Furthermore, the graphene based electro optical modulator behaves like an intrinsic broadband semiconductor without any resonant optical effect[51]. Therefore, in comparison to compound semiconductors a graphene based electro optical modulator has strong light interaction properties [51]. With many more advantages, electro optical modulator based on graphene material can open promising opportunities to integrate photonic applications with a solid footprint, low voltage and ultra-fast modulation for a broad and wide range of different wavelength[23, 51] .

Chapter 6

Conclusion

6.1 Thesis Conclusion

In our experiment we have developed a two-dimensional surface conductivity material model for graphene for our simulations[23]. We calculated intra-band conductivity analytically and inter-band conductivity numerically using Lumerical FDTD. We are able to plot real and imaginary surface conductivity graph. We find that, numerical data is match with analytical data which shows that, graphene has high surface conductivity.

We also demonstrated the surface plasmon polariton of graphene based plasmonic waveguides by using different structures of TE and TM polarized surface plasmon waveguides [23]. In surface plasmon polariton first we excite a s-polarized surface plasmon where we take incident angle analytically. Then from Lumerical FDTD, we find the numerical angle. Here both the incident angle is a matched. In the reflected power, we observed a is dip which is due to evanescent wave. Because, evanescent wave excites the surface plasmon, and the reflected power decreases with the increase of source angle. We also find that, source angle for surface plasmon is greater than the total internal reflection angle[23]. Moreover, we also demonstrated very high electric field intensity occurs at source angle for spp.

Then we excite a p-polarized surface plasmon where we choose 3 different substrates (Glass, Si, Ti) for this. For the glass, we find match in source angle for both numerical and analytical values and we saw dip in the reflected power around the source angle due to evanescent wave. Total internal reflection is less than the source angle. We also find, electric intensity is very high around the source angle. But for the Ti and Si, we don’t find ant match between

numerical and analytical values. Electric intensity is also not that high around the source angle. So, both Ti and Si substrate is not perfect for graphene P-polarization. Also, there is no dip in reflected power around the source angle. So, surface plasmon excitation is very week. Therefore, using a glass substrate in p-polarized surface plasmon gives us strongest excitation.

After that we demonstrate constant absorption rate using Lumerical FDTD setup where we find absorption coefficient vs frequency graph. At first, absorption is very high but after gradual frequency increase, absorption is gradually decrease and then increase and become constant at .023(2.3%).

Then we showed the complete light absorption in periodically patterned graphene nanodisk. For the total light absorption, we will take dielectric graphene coatings of various thicknesses. For the various thicknesses, we find the graph of Photon Energy (ev) vs absorbance. After comparing different graph for different thicknesses, we find when the dielectric layer thickness is 800nm, we find best absorbance. The SPR peak is very close for different dielectric thicknesses in between .124 to .131 Ev. If we observe the reflection curve for 800nm dielectric coating, we find prominent absorption dip around the wave length of 9705nm. So, in near infrared light, energy is absorbed by surface plasmon.

Finally, we have built an electro-optical modulator device based on graphene coated waveguide material where we showed we can achieve the absorption and transmission by changing the chemical potential or fermi energy level of graphene[54]. For optical simulation result we use both electrical and optical simulation and we get a plot for electro optical response. From the electro optical plot, we can see transmission and absorption change at different gate voltages.

- For V<-1V energy transmission is High

- For -1<V<3.8 energy transmission is Low and absorbance is high
- For V>3.8V energy transmission is High

Therefore, from the observation we can say that, we can control the photon energy absorption and transmission by changing the fermi energy level of graphene layer[54].

On the other hand, for electrical simulation we doped Si wave guide with Boron and apply different bias voltage. We find changes in Chemical potential/ fermi level of Graphene sheet at different bias voltages. From the plot we can see that the chemical potential of graphene layer is very high at the beginning and decrease with the increase of bias voltage. So, when we change the Fermi level for different bias voltage the chemical potential also changes.

The Electro- Optical modulator based on graphene coated waveguide shows that

- At a lower biased voltage, we get a strong absorption
- Optical absorption is independent of wavelength
- It behaves like intrinsic broadband without any resonant optical effect

Therefore, these results from optical and electrical performance of graphene-based surface plasmon polariton of plasmonic waveguide and devices shows that we can model any device where we need to control the absorption and transmission rate of photon with the help of graphene.

6.2 Future works

Graphene has a huge potential and almost many of its potentials are untouched. We studied on the fundamental of graphene-based waveguide and devices. In future, we are looking forward to work on various graphene based real-life applications like bio sensors, nano chips technology, optical communications, conductors and many more.

In our surface plasmon polariton part, in P- polarization we work with 3 substrates, glass, Ti, Si. We think in the future, some other substrates should be paired with graphene and see the

effects on their reflected and transmitted power and surface plasmon excitation. Then in our optical absorption in periodically patterned graphene part, we find out the prominent thickness for total light absorption, and based on the thickness further work can be done in tunable photo detector, broad spectrum photo absorption sectors. Moreover, in our electro-optical modulator (EOM) based on graphene material part, we try to review the connection in between Fermi level, bias voltage, and chemical potential. For the future, we think other semiconductor material Ge, GaAs can be further examined to observe their properties.

However, graphene has a huge potential and almost many of its potentials are untouched. We study on the fundamental of graphene-based waveguide and devices. In future, we can work on various graphene based real-life applications like bio sensors, nano chips technology, optical communications, conductors and many more.

References

[1] A. K. Geim and K. S. Novoselov, "The rise of graphene," vol. 6, 2009, pp. 11-19.

[2] G. Yang, L. Li, L. W.B, and M. Ng, "Structure of graphene and its disorders: a review," *Science and Technology of Advanced Materials,* vol. 19, pp. 613-648, 08/29 2018.

[3] A. D. Ghuge, A. R. Shirode, and V. J. Kadam, "Graphene: A Comprehensive Review," (in eng), *Curr Drug Targets,* vol. 18, no. 6, pp. 724-733, 2017.

[4] E. Celasco *et al.*, "Handbook of Graphene," 08/01 2019.

[5] I. Sadegh Amiri, M. Ariannejad, V. Sorger, and P. Yupapin, "Silicon microring resonator waveguide-based graphene photodetector," *Microsystem Technologies,* 06/28 2018.

[6] O. J. Dada, *Electronic and Dielectric Properties of Graphene and Graphene Oxide : Superior Electronic and Dielectric Properties of Corrugated Electrochemically Reduced Graphene over Graphene Oxide Paper*. 2020.

[7] S. Bharech and R. Kumar, "A Review on the Properties and Applications of Graphene," *Journal of Material Science and Mechanical Engineering (JMSME),* vol. 2, pp. 70-73, 05/30 2015.

[8] S. K. Vashist and J. Luong, "Recent advances in electrochemical biosensing schemes using graphene and graphene-based nanocomposites," *Carbon,* vol. 84, 04/30 2015.

[9] D. Persano Adorno, L. Bellomonte, and N. Pizzolato, "The amazing graphene: An educational bridge connecting different physics concepts," *European Journal of Physics,* vol. 39, 10/06 2017.

[10] X. Zhou, W. Wang, and Z. Liu, "Graphene Overview," 2014, pp. 1-20.

[11] A. R. Sadrolhosseini, M. Habibiasr, S. Shafie, H. Solaimani, and H. N. Lim, "Optical and Thermal Properties of Laser-Ablated Platinum Nanoparticles Graphene Oxide Composite," (in eng), *Int J Mol Sci,* vol. 20, no. 24, Dec 6 2019.

[12] S. Saha and E. Graham, "Non-steroidal Anti-inflammatory Drugs," 2016, pp. 285-292.

[13] S. Thongrattanasiri, F. H. L. Koppens, and F. J. García de Abajo, "Complete Optical Absorption in Periodically Patterned Graphene," *Physical Review Letters,* vol. 108, no. 4, p. 047401, 01/27/ 2012.

[14] E. Solati and D. Dorranian, "Nonlinear optical properties of the mixture of ZnO nanoparticles and graphene nanosheets," *Applied Physics B,* vol. 122, 04/01 2016.

[15] P. B. Johnson and R. W. Christy, "Optical Constants of the Noble Metals," *Physical Review B,* vol. 6, no. 12, pp. 4370-4379, 12/15/ 1972.

[16] O. Zabihi *et al.*, "A sustainable approach to scalable production of a graphene based flame retardant using waste fish deoxyribonucleic acid," *Journal of Cleaner Production,* vol. 247, p. 119150, 11/01 2019.

[17] H. Wang, H. Zhao, G. Hu, S. Li, H. Su, and J. Zhang, "Graphene Based Surface Plasmon Polariton Modulator Controlled by Ferroelectric Domains in Lithium Niobate," *Scientific Reports,* vol. 5, p. 18258, 12/14 2015.

[18] M. Rhouma, M. Oueslati, and B. Guizal, "Surface plasmons on a doped graphene sheet with periodically modulated conductivity," *Superlattices and Microstructures,* vol. 96, 05/01 2016.

[19] K. Bliokh, F. Rodríguez-Fortuño, A. Bekshaev, Y. Kivshar, and F. Nori, "Electric current induced unidirectional propagation of surface plasmon-polaritons," *Optics Letters,* vol. 43, 12/01 2017.

[20] M. Heydari and M. Samiei, *Plasmonic Graphene Waveguides: A Literature Review.* 2018.

[21] M. Bordag and I. Pirozhenko, "Surface plasmons for doped graphene," *Physical Review D,* vol. 91, 02/02 2015.
[22] S. s. Dukhin, R. Zimmermann, and C. Werner, "Surface Conductivity," 2012, pp. 95-126.
[23] J. Pond *et al.*, *Modeling graphene based surface plasmon waveguides and devices*. 2016, p. 97501A.
[24] W. Liang, Z. Li, Y. Wang, W. Chen, and Z. Li, "All-angle optical switch based on the zero reflection effect of graphene–dielectric hyperbolic metamaterials," *Photonics Research,* vol. 7, p. 318, 03/01 2019.
[25] F. Majeed, T. Fickenscher, M. Shahpari, and D. Thiel, "Measurement of surface conductivity of graphene at W-band," *Microwave and Optical Technology Letters,* vol. 61, 03/13 2019.
[26] R. Bala, A. Marwaha, and S. Marwaha, "Mathematical formulation of surface conductivity for graphene material," *Journal of Engineering Science and Technology,* vol. 12, pp. 1677-1684, 06/01 2017.
[27] N. Miura, P. Elumlai, V. V. Plashnitsa, T. Ueda, R. Wama, and M. Utiyama, "Solid State Gas Sensing," *Solid-state Electrochemical Gas Sensing,* pp. 181-190, 01/01 2009.
[28] I. Degli-Eredi, J. Sipe, and N. Vermeulen, "TE-polarized graphene modes sustained by photonic crystal structures," *Optics letters,* vol. 40, pp. 2076-9, 05/01 2015.
[29] I. Degli-Eredi, J. Sipe, and N. Vermeulen, *Graphene-covered 1D photonic crystals enabling TE-polarized graphene modes*. 2016, p. 98850H.
[30] K. A. Tarumaraja *et al.*, "FDTD numerical analysis of SPR sensing using graphene-based photonic crystal," pp. 79-81, 2016.
[31] M. Weik, "Communications Standard Dictionary," 01/01 1996.
[32] M. Ukhtary and R. Saito, "Quantum Description of Surface Plasmon Excitation by Light in Graphene," *physica status solidi (b),* vol. 255, p. 1800181, 08/23 2018.
[33] A. Sharma, "Plasmonics-Based Fiber Optic Sensors," vol. 21, 2017, pp. 51-67.
[34] D. Mason, S. Menabde, and N. Park, "Unusual Otto excitation dynamics and enhanced coupling of light to TE plasmons in graphene," *Optics express,* vol. 22, pp. 847-58, 01/13 2014.
[35] F. Ramos-Mendieta, J. Hernández-López, and M. Palomino-Ovando, "Transverse magnetic surface plasmons and complete absorption supported by doped graphene in Otto configuration," *AIP Advances,* vol. 4, p. 067125, 06/01 2014.
[36] D. Mason, S. Menabde, and N. Park, *Enhanced coupling of light to TE plasmons in multilayer graphene*. 2014.
[37] S. Malthesh, P. Prajwal, N. Praveen, and N. Krishnaswamy, *Modeling and Analysis of Micro-ring Resonator for Bio-sensing Applications*. 2018, pp. 2418-2421.
[38] L. Wang, L.-G. Wang, and M. Zubairy, "Tunable positive and negative group delays of light reflection from layer structures with a graphene layer," *Journal of Applied Physics,* vol. 122, p. 115301, 09/21 2017.
[39] J. Chi, H. Liu, N. Huang, and Z. Wang, "A broadband enhanced plasmonic modulator based on double-layer graphene at mid-infrared wavelength," *Journal of Physics D: Applied Physics,* vol. 52, 07/30 2019.
[40] S. Rakheja and P. Sengupta, "The tuning of light-matter coupling and dichroism in graphene for enhanced absorption: Implications for graphene-based optical absorption devices," *Journal of Physics D: Applied Physics,* vol. 49, 06/13 2015.
[41] S. Thongrattanasiri, F. Koppens, and J. Garcia de Abajo, "Complete Optical Absorption in Periodically Patterned Graphene," *Physical review letters,* vol. 108, p. 047401, 01/27 2012.

[42] G. Gómez-Santos and T. Stauber, "Graphene plasmons and retardation: Strong light-matter coupling," *Europhysics Letters (epl),* vol. 99, 04/26 2012.
[43] K. F. Mak, M. Y. Sfeir, Y. Wu, C. H. Lui, J. A. Misewich, and T. F. Heinz, "Measurement of the Optical Conductivity of Graphene," *Physical Review Letters,* vol. 101, no. 19, p. 196405, 11/07/ 2008.
[44] F. H. L. Koppens, D. E. Chang, and F. J. García de Abajo, "Graphene Plasmonics: A Platform for Strong Light–Matter Interactions," *Nano Letters,* vol. 11, no. 8, pp. 3370-3377, 2011/08/10 2011.
[45] D. V. van Coevorden, R. Sprik, A. Tip, and A. Lagendijk, "Photonic Band Structure of Atomic Lattices," *Physical Review Letters,* vol. 77, no. 12, pp. 2412-2415, 09/16/ 1996.
[46] H.-J. Kim, K.-J. Seo, and D.-E. Kim, "Investigation of mechanical behavior of single- and multi-layer graphene by using molecular dynamics simulation," *International Journal of Precision Engineering and Manufacturing,* vol. 17, pp. 1693-1701, 12/01 2016.
[47] M. Pu *et al.,* "Strong enhancement of light absorption and highly directive thermal emission in graphene," *Optics express,* vol. 21, pp. 11618-27, 05/20 2013.
[48] M. Alsawafta, M. Wahbeh, and V.-V. Truong, "Simulated Optical Properties of Gold Nanocubes and Nanobars by Discrete Dipole Approximation," *Journal of Nanomaterials,* vol. 2012, 01/01 2012.
[49] V. Ryzhii *et al.*, *Graphene-based electro-optical modulator: Concept and analysis*. 2012.
[50] A. Bain and P. Chand, "Ferroelectric Ceramics: Devices and Applications," 2017, pp. 195-306.
[51] M. Liu *et al.,* "A graphene-based broadband optical modulator," (in eng), *Nature,* vol. 474, no. 7349, pp. 64-7, Jun 2 2011.
[52] E. O. Polat and C. Kocabas, "Broadband optical modulators based on graphene supercapacitors," (in eng), *Nano Lett,* vol. 13, no. 12, pp. 5851-7, 2013.
[53] L. Ji *et al.*, "Design of an Electro-Absorption Modulator Based on Graphene-on-Silicon Slot Waveguide," *IEEE Photonics Journal,* vol. PP, pp. 1-1, 05/22 2019.
[54] S. Luo, Y. Wang, X. Tong, and Z. Wang, "Graphene-based optical modulators," (in eng), *Nanoscale Res Lett,* vol. 10, p. 199, 2015.
[55] Q. Bao and K. Loh, "Graphene Photonics, Plasmonics, and Broadband Optoelectronic Devices," *ACS nano,* vol. 6, pp. 3677-94, 04/18 2012.
[56] G. Wang, X. Liu, H. Lu, and C. Zeng, "Graphene plasmonic lens for manipulating energy flow," *Scientific reports,* vol. 4, p. 4073, 02/12 2014.
[57] T. Linlong *et al.*, "Complete optical absorption in graphene by using nano-gratings to excite graphene surface plasmons," *Microelectronic Engineering,* vol. 145, 09/01 2015.
[58] M. Fu *et al.,* "Efficient terahertz modulator based on photoexcited graphene," *Optical Materials,* vol. 66, pp. 381-385, 04/01 2017.
[59] Y. Choi, J. M. Yoo, and B. Hong, "Structure and properties of graphene," 2020, pp. 5-26.
[60] F. Wang *et al.*, "Gate-Variable Optical Transitions in Graphene," *Science (New York, N.Y.),* vol. 320, pp. 206-9, 05/01 2008.
[61] S. Zhou *et al.*, "First direct observation of Dirac fermions in graphite," *Nature Physics,* vol. 2, 09/02 2006.
[62] J. Yao, Y. Chen, L. Ye, N. Liu, G. Cai, and Q. Liu, "Multiple resonant excitations of surface plasmons in a graphene stratified slab by Otto configuration and their independent tuning," *Photonics Research,* vol. 5, p. 377, 08/01 2017.

[63] A. Liu *et al.*, "A high-speed silicon optical modulator based on a metal-oxide-semiconductor capacitor," *Nature*, vol. 427, pp. 615-8, 03/01 2004.